2022

Effect of reduction methods on the properties of composite films of bacterial cellulose-silver nanoparticles

Ratchanon Jenkhongkarn
Faculty of Engineering

EFFECT OF REDUCTION METHODS ON THE PROPERTIES OF COMPOSITE FILMS OF BACTERIAL CELLULOSE-SILVER NANOPARTICLES

Mr. Ratchanon Jenkhongkarn

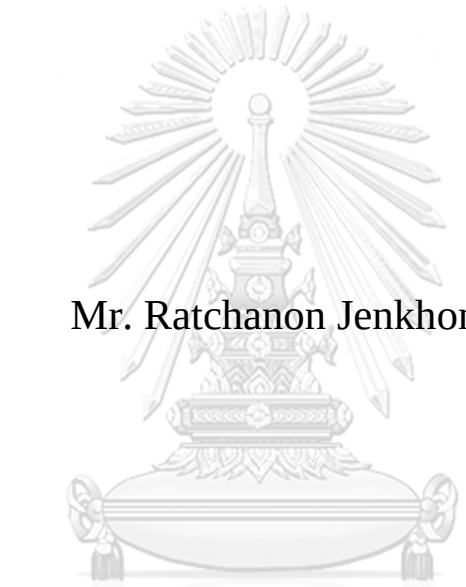

A Thesis Submitted in Partial Fulfillment of the Requirements
for the Degree of Master of Engineering in Chemical Engineering
Department of Chemical Engineering
FACULTY OF ENGINEERING
Chulalongkorn University
Academic Year 2022

ผลของวิธีรีดิวซ์ต่อคุณสมบัติของฟิล์มคอมโพสิตของ แบคทีเรียลเซลลูโลสและอนุภาคซิลเวอร์นาโน

นายรัชชานนท์ เจนคล่องการ

วิทยานิพนธ์นี้เป็นส่วนหนึ่งของการศึกษาตามหลักสูตรปริญญาวิศวกรรมศาสตรมหาบัณฑิต
สาขาวิชาวิศวกรรมเคมี ภาควิชาวิศวกรรมเคมี
คณะวิศวกรรมศาสตร์ จุฬาลงกรณ์มหาวิทยาลัย
ปีการศึกษา 2565

Thesis Title	EFFECT OF REDUCTION METHODS ON THE PROPERTIES OF COMPOSITE FILMS OF BACTERIAL CELLULOSE-SILVER NANOPARTICLES
By	Mr. Ratchanon Jenkhongkarn
Field of Study	Chemical Engineering
Thesis Advisor	Professor MUENDUEN PHISALAPHONG, Ph.D.

Accepted by the FACULTY OF ENGINEERING, Chulalongkorn University in Partial Fulfillment of the Requirement for the Master of Engineering

..... Dean of the FACULTY OF ENGINEERING
(Professor SUPOT TEACHAVORASINSKUN, D.Eng.)

THESIS COMMITTEE

..... Chairman
(Professor ANONGNAT SOMWANGTHANAROJ, Ph.D.)

..... Thesis Advisor
(Professor MUENDUEN PHISALAPHONG, Ph.D.)

..... Examiner
(Professor BUNJERD JONGSOMJIT, Ph.D.)

..... External Examiner
(Assistant Professor Suchata Kirdponpattara, D.Eng.)

รัชชานนท์ เจนคล่องการ : ผลของวิธีรีดิวซ์ต่อคุณสมบัติของฟิล์มคอมโพสิตของ แบคทีเรียลเซลลูโลสและอนุภาคซิลเวอร์นาโน. (EFFECT OF REDUCTION METHODS ON THE PROPERTIES OF COMPOSITE FILMS OF BACTERIAL CELLULOSE-SILVER NANOPARTICLES) อ.ที่ปรึกษาหลัก : ศ. ดร.เหมือนเดือน พิศาลพงศ์

คอมโพสิตฟิลม์ระหว่าง แบคทีเรียลเซลลูโลสและอนุภาคซิลเวอร์นาโน ได้ถูกทำการเตรียมโดยใช้วิธีการรีดิวซ์ซิลเวอร์จากภายในวิธีต่างๆ โดยประกอบด้วยการใช้ โซเดียมไฮดรอกไซด์, กรดแอสคอร์บิก, ไคโตซาน และรังสียูวี โดยได้มีการทำศึกษาผลของวิธีรีดิวซ์ต่อคุณสมบัติต่างๆของตัวฟิล์มคอมโพสิต คอมโพสิตที่ถูกรีดิวซ์ด้วยไคโตซานมีการกระจายของอนุภาคซิลเวอร์นาโนภายในโครงสร้างนาโนเซลลูโลสดี และมีขนาดอนุภาคเล็กที่สุด โดยคอมโพสิตที่ถูกรีดิวซ์ด้วยกรดแอสคอร์บิกมีขนาดอนุภาคใหญ่ที่สุด การใส่อนุภาคซิลเวอร์นาโนลงไปในคอมโพสิตโดยส่วนใหญ่แล้วจะลดความเป็นผลึกของคอมโพสิต ยกเว้นคอมโพสิตที่ถูกรีดิวซ์ด้วยกรดแอสคอร์บิกที่มีค่าความเป็นผลึกเพิ่มขึ้น การทดสอบคุณสมบัติทางกลแสดงให้เห็นว่าคอมโพสิตที่ถูกรีดิวซ์ด้วยกรดแอสคอร์บิกมีค่ามอดูลัสของยังสูงที่สุด โดยมีค่าถึง 8960 เมกะปาสกาล และคอมโพสิตที่ถูกรีดิวซ์ด้วยรังสียูวี มีค่าความทนแรงดึงและค่าการยืดตัว ณ จุดขาดสูงที่สุด การทดสอบคุณสมบัติทางความร้อนพบว่า อุณหภูมิการเปลี่ยนสถานะคล้ายแก้วและ อุณหภูมิสลายตัวของคอมโพสิตมีค่าคล้ายกับแบคทีเรียลเซลลูโลส โดยมีขั้นการสลายตัวเพิ่มขึ้นที่อุณหภูมิสูง คอมโพสิตที่ถูกรีดิวซ์ด้วยโซเดียมไฮดรอกไซด์มีค่าการนำไฟฟ้าสูงสุดที่ 1.1×10^{-7} ซีเมนต์ต่อเซ็นติเมตร ความสามารถในการดูดซับน้ำของคอมโพสิตลดลงจากการใส่อนุภาคซิลเวอร์ ยกเว้นคอมโพสิตที่ถูกรีดิวซ์ด้วยไคโตซานที่มีค่าการดูดซับน้ำเพิ่มขึ้นโดยมีค่า 344% คอมโพสิตระหว่างแบคทีเรียลเซลลูโลสและอนุภาคซิลเวอร์นาโน แสดงคุณสมบัติในการต่อต้านเชื้อแบคทีเรียอย่างสูงต่อ เชื้อเอสเชอริเคียโคไลและ เชื้อสแตปฟิโลคอคคัส ออเรียส ผลการทดลองเหล่านี้แสดงให้เห็นถึงศักยภาพของการนำฟิลม์คอมโพสิตระหว่างแบคทีเรียลเซลลูโลสและอนุภาคซิลเวอร์นาโนไปใช้งานในการใช้งานเป็นแผ่นแปะแผล ไบโอเซนเซอร์ หรือใช้งานด้านอื่นๆ

สาขาวิชา	วิศวกรรมเคมี	ลายมือชื่อนิสิต .....
ปีการศึกษา	2565	ลายมือชื่อ อ.ที่ปรึกษาหลัก .....

6370247721 : MAJOR CHEMICAL ENGINEERING
KEYWOR D: bacterial cellulose, silver nanoparticle, biocomposite film

Ratchanon Jenkhongkarn : EFFECT OF REDUCTION METHODS ON THE PROPERTIES OF COMPOSITE FILMS OF BACTERIAL CELLULOSE-SILVER NANOPARTICLES . Advisor: Prof. MUENDUEN PHISALAPHONG, Ph.D.

Composite films of bacterial cellulose-silver nanoparticles (BC-Ag) were prepared by different methods of *in-situ* reduction of silver, using sodium hydroxide, ascorbic acid, chitosan, and UV irradiation. The effects of the reduction methods on their properties were investigated. The chitosan-reduced composite exhibited dispersed silver nanoparticles (AgNPs) within the nanocellulose matrix with the smallest size, while the ascorbic-reduced composite displayed the largest size. The incorporation of AgNPs tended to reduce the crystallinity of the composites, except for the ascorbic-reduced composite which exhibited an increase in crystallinity. Mechanical testing revealed that the ascorbic-reduced composite had the highest Young's modulus of 8960 MPa, whereas the UV-reduced composite had the highest tensile strength and elongation at break. Thermal analysis of BC-Ag composites indicated similar glass transition temperature and decomposition profiles to BC, with additional weight loss steps at high temperatures. The sodium hydroxide-reduced composite demonstrated the highest electrical conductivity of 1.1×10^{-7} S/cm. Water absorption capacity was reduced by the incorporation of AgNPs, except for the chitosan-reduced composite, which showed an enhanced water absorption capacity of 344%. All BC-Ag composites displayed very strong antibacterial activities against *Escherichia coli* and *Staphylococcus aureus*. These results also highlight the potential uses of BC-Ag composites in various applications, including wound healing and biosensors.

Field of Study:	Chemical Engineering	Student's Signature .....
Academic Year:	2022	Advisor's Signature .....

ACKNOWLEDGEMENTS

I would like to express my sincere gratitude to Prof. Muenduen Phisalaphong for her unwavering support, invaluable guidance, and exceptional expertise throughout the completion of this thesis. Her insightful feedback and constructive criticism have profoundly influenced my research journey and significantly broadened my perspectives. I am deeply honored to have had Prof. Phisalaphong as my advisor, and I am certain that the lessons learned from her will continue to shape my career.

In addition, I am grateful for my thesis committee: Prof. Anongnat Somwangthanaroj (Chairman), Prof. Bunjerd Jongsomjit (Examiner), and Asst.Prof. Suchata Kirdponpattara (External examiner) for generously dedicating their time to serve as my committee member.

Lastly, I would like to express my sincere thanks to all my seniors and friends from the Chemical Engineering Department at Chulalongkorn University for their unwavering support and valuable advice. Their encouragement and camaraderie have been invaluable throughout this journey.

Ratchanon Jenkhongkarn

TABLE OF CONTENTS

Page

LIST OF TABLES

Page

LIST OF FIGURES

Page

CHAPTER ONE: INTRODUCTION TO THE STUDY

1.1 Introduction and Background

Cellulose is one of the most abundant, readily available, and inexpensive common polymers on earth with an annual production of around 75 billion tons [1]. Cellulose offers significant advantages over petroleum-derived polymers, as it is renewable, environmentally friendly, cost-efficient, non-toxic, biodegradable, and biocompatible [2-4]. Apart from plants, several microorganisms are known to be a producer of cellulose. Bacterial cellulose (BC), produced by bacteria differs from plant cellulose as it lacks hemicellulose, lignin, and other compounds present in plant cellulose.

BC can be produced by several bacteria, particularly *Gluconacetobacter xylinus*, and has shown tremendous potential. BC exhibits remarkable properties, including high purity, high crystallinity, water-holding capacity, excellent mechanical properties, large surface area, and good biocompatibility and biodegradability [5]. These exceptional characteristics make BC a suitable material for various applications, such as tissue engineering, electronic devices, biomedical applications, and drug delivery systems. In the biomedical field, BC serves as a wound dressing material, artificial skin, vascular grafts, scaffold for tissue engineering, artificial blood vessel, and medical pads [6, 7]. BC has also been utilized as a temporary substitute for burn victims' skin [8], an environmentally compatible ion exchange membrane in fuel cells [9], and as biocompatible and biodegradable sensors and actuators [10]. However, modifications are necessary to enhance the capabilities and improve the properties of BC materials before they can be effectively utilized in various applications. For instance, pure BC lacks electrical conductivity, magnetism, and hydrophobicity [11]. Therefore, BC cannot be used directly in electrical devices, batteries, sensors, or electrochromic devices [8, 11]. Moreover, BC does not possess inherent antimicrobial properties [12], and despite its high mechanical properties, its stress-bearing capacity is impeded due to numerous pores [2]. However, due to its structural characteristics, BC exhibits significant potential as a matrix and reinforcement in composite materials [13]. Recently, different types of BC composites have been synthesized, resulting in enhanced mechanical, biological, and electrical properties [2, 14]. Various methods have been employed to improve the properties of BC, including modifications to the synthesis method, culture conditions, and the incorporation of BC with other materials to create a different type of BC composite [15, 16], which can widen the application of BC in many other areas.

Silver, in the form of nanoparticles (AgNPs) and oxides (mainly Ag_2O), has been widely used for antibacterial applications. The unique physicochemical properties of nanosilver, including its high surface-to-volume ratio and inherent biocidal activity, make them promising candidates for combating bacterial infections [17]. However, for practical application, silver needs to be integrated into composites or retained inside solid support to apply over the affected area, preventing rapid oxidation and increasing its stability [18]. BC contains abundant hydroxyl groups that

are capable of reducing Ag^+ to Ag^0 [19] and offers an ideal matrix for silver integration due to its porous and interconnected structure. BC could act as both a reducing agent and stabilizing agent in the reduction of silver ions to silver nanoparticles [19]. As a result, there has been significant research dedicated to investigating the incorporation of silver into BC to develop composite materials with enhanced antimicrobial activity and excellent mechanical properties. Several research studies have explored various reduction methods to convert silver ions into silver nanoparticles within the BC matrix. However, previous studies have primarily focused on investigating the antibacterial properties of bacterial cellulose-silver nanoparticles (BC-Ag) composites, neglecting the investigation of other properties. Furthermore, the effects of different reduction methods on the final properties of the composite have rarely been compared.

This research aims to investigate the influences of different methods of *in-situ* reduction of silver nitrate in nanocellulose matrix on the properties of BC-Ag composite films using facile, cheap, and easily replicable approaches. The methods applied in this study include the chemical reduction using sodium hydroxide (NaOH), ascorbic acid ($C_6H_8O_6$), and chitosan solutions and photochemical reduction using UV irradiation. The BC and BC-Ag composites were characterized using various techniques, including X-ray diffraction (XRD), field emission scanning electron microscope (FE-SEM), Fourier transform infrared spectra (FT-IR), universal testing machine (UTM), electrochemical impedance spectroscopy (EIS), as well as thermal analysis techniques, which include thermogravimetric analysis (TGA) and differential scanning calorimetry (DSC). Additionally, the antibacterial activities of BC-Ag composites were evaluated using the colony forming count method against gram-positive bacteria (*S. aureus*) and gram-negative bacteria (*E. coli*).

1.2 Research objectives

The purpose of the study is to investigate the effects of different methods of in-situ reduction of silver nitrate in a nanocellulose matrix on the properties of BC-Ag composite films, finding the effect of the incorporation of Ag on the physical, chemical, electrical, and biological properties of the composite films.

1.3 Scope and Limitations of the Study

1.3.1 Study the effect of the reduction method of silver nitrate on the properties BC-Ag composites. These methods include chemical reduction utilizing sodium hydroxide, ascorbic acid, and chitosan solutions, as well as photochemical reduction using UV irradiation. The final properties of the BC-Ag composites were compared with pristine BC and between each reduction method.

1.3.2 BC were biosynthesized BC a 14.5 cm diameter sterile vessels with 75 mL total liquid volume under static incubation at 30 °C for 7 days. BC-Ag reduced by sodium hydroxide, ascorbic acid, and UV irradiation were immersed in 0.02 M $AgNO_3$ and BC-Ag reduced by chitosan were immersed in 0.02 M $AgNO_3$, 2.0% (w/v) chitosan, and 1.0% (v/v) acetic acid solution. The immersion time for all methods was 2 days. For the reduction of silver nitrate

using sodium hydroxide and ascorbic acid, a concentration of 0.12 M of sodium hydroxide and ascorbic acid was used with a total reaction time of 30 min. For the reduction using chitosan, the temperature used in the heating process was 75 ± 2 °C with a duration of 5 h. For the reduction using UV irradiation, UV light (wavelength of 254 nm, 15 W) was used, with an irradiation time of 5 h.

1.3.3 Characterization of physical, chemical, and electrical properties of BC and BC-Ag composites was done using X-ray diffraction (XRD), field emission scanning electron microscope (FE-SEM), Fourier transform infrared spectra (FT-IR), universal testing machine (UTM), electrochemical impedance spectroscopy (EIS), thermogravimetric analysis (TGA) and differential scanning calorimetry (DSC). The antibacterial activity was assessed by the colony forming count method against gram-positive bacteria (*S. aureus*) and gram-negative bacteria (*E. coli*).

1.4 Expected benefits

1.4.1 Widen the application potential of BC by improving its properties through the incorporation of silver nanoparticles. By enhancing the capabilities of BC materials, they can be effectively utilized in diverse areas such as tissue engineering, biomedical applications, electronic devices, drug delivery systems, and more.

1.4.2 By comparing the effects of different *in-situ* reduction methods. This analysis can provide valuable insights into the most effective and efficient method for incorporating silver nanoparticles into the BC matrix for each application, contributing to future research and practical applications.

CHAPTER TWO: REVIEW OF THE LITERATURE

2.1 Bacterial cellulose (BC)

Cellulose is one of the most abundant biomaterials on Earth, which is also biodegradable, renewable, and has been known for its high potential as a raw material in the fabrication of various composites. Cellulose-based composites can be modified to be excellent in both properties and environmentally friendly aspects.

One alternative source of cellulose is bacterial cellulose (BC), which can be produced from several microorganisms such as bacteria, fungi, and algae. One of which is the acetic acid-producing bacteria named *Gluconacetobacter xylinus* (formerly *Acetobacter xylinum*) [20]. The Gram-negative strain *G. xylinus* is one of the most efficient sources for the production of BC and is the most widely used strain industrially because of its ability to metabolize many types of carbon/nitrogen sources [21]. Chemically, BC is the same as plant cellulose. But unlike natural cellulose products from plants, the cellulose produced from microbial strains is pure and free of hemicellulose, lignin, pectin, or any other compounds, which normally present in plant pulp [2]. Moreover, BC also has a distinctive ultrafine three-dimensional network of cellulose fibers [22]. Compared to plant-based cellulose, BC can be obtained in higher purity because of the absence of lignin and hemicellulose, with a higher crystallinity index, and better mechanical properties [11]. Due to said properties and superior properties compared to plant-based cellulose, combined with its excellent mechanical properties, water-holding capacity, biocompatibility, and biodegradability [23], BC is preferable to plant-based cellulose in fabricating electrically conductive composites and other applications [24], and has received considerable attention and has found its application in various fields.

During the BC synthesis process, glucose chains are produced inside the bacteria body and are extruded through small pores on its cell envelope [11]. Then microfibrils are formed from the glucose chain which are aggregated further to form cellulose ribbons [23], the ribbons of nanofibers then generated a structure of a web-shaped network with a gap between the fibers itself. The nano-fibrils of BC create an expanded surface area with and highly porous matrix [25]. The combination of purity, well-arranged fibers, extended surface area, and variable pore geometry has imparted BC with many exceptional properties [13]. A random distribution of cellulose fibers of BC can be seen by utilizing a scanning electron microscope (SEM) [13]. BC end applications usually depend on its properties such as mechanical properties, thermal properties, water holding capacity, and electrical properties. All of these properties depend on its structural features including the arrangement of BC microfibrils and the structure of the porous matrix [2]. Various parameters during fermentation such as types of bacterial strain, fermentation medium, carbon sources, fermentation duration, and synthesis method can also affect these structural features [2].

2.2 Applications and Limitations BC

Because of BC outstanding properties, there have been multiple attempts to utilize BC in multiple commercial products. Commercial items utilizing BC include high-performance speaker diaphragms, headphone membranes, high-grade paper, and textiles [26]. And in the biomedical field, BC are used as a wound dressing material [7], artificial skin, vascular grafts, scaffold for tissue engineering, artificial blood vessel, and medical pads [6]. BC is used as a temporary skin substitution for burns victims [8], as an environmentally compatible ion-exchange membrane for fuel cells [9], and as a biocompatible and biodegradable sensors and actuators [10].

However, modifications are required for BC to enhance the capabilities and properties of the BC materials before being used in different applications. For example, pure BC lacks electrical conductivity, optical transparency, magnetism, and hydrophobicity [2]. Meaning that BC cannot be used directly in electrical devices, batteries, sensors, or electrochromic devices [8]. BC also has no antimicrobial properties [12] and due to its numerous pores, despite its high mechanical properties, the stress-bearing capabilities are hindered [2].

2.3 Composite material

Composite is a combination of two types of individual parts, which are the matrix and the reinforcement materials. The main component usually acts as a continuous matrix, while the other component serves as a reinforcement [27]. imparting physio-chemical and biological properties to the matrix [11]. The wide range of materials for matrix and reinforcement materials allows the synthesis of various composites with various properties.

2.3.1 Need for BC composite

The deficiencies of the pristine BC mentioned above restrict its ability to be utilized in various fields, thus providing the demand for the synthesis of BC composite. Because of its structural features, BC has a high potential to act as a matrix and a reinforcement in composite materials [13]. Different types of composites of BC have been synthesized in the past year, enhancing its various properties such as mechanical properties, biological properties, and electrical properties. BC composite incorporated with conducting material has also been used in electric and magnetic devices [11]. A diagram of BC being utilized with various materials to create BC composites and its uses in different applications are illustrated in Figure 1**.**

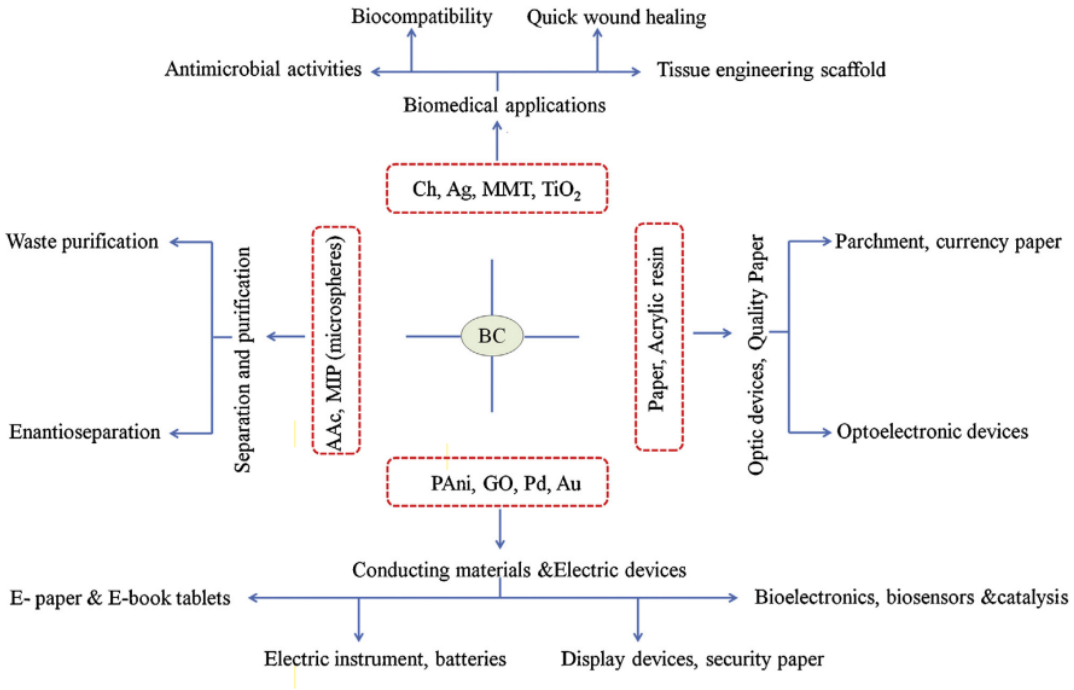

Figure 1. Diagram of BC being utilized with various materials and its uses in different applications [11]

2.3.2 Cellulose role in conductive composite

Despite cellulose by itself being a bad conductor of electricity, the cellulosic ingredient in the composite usually serves as a reinforcement due to the high crystallinity properties of the materials [28], acting as a mechanical support for the conductive material, serving as a stable dimension. BC has been explicitly used in the preparation of electrically conductive composites [24]. For example, Feng, Zhang [29] created a layered structure of BC and graphene oxide with a vacuum, in which the graphene oxide contributed to the mechanical strength of the material in addition to electrical conductance. One of the advantageous attributes of cellulose, as a support for conductive materials, is dimensional stability provided, especially in lengthwise dimension [24]. Cellulose fibers typically swell or shrink by a small percentage in various humidity conditions [30], which might be important for supporting a fragile conductive material.

2.4 Culture methods of BC

There are several methods for the production of BC such as static, agitated, and bioreactor. Different culture methods can result in different morphology, structure, and properties of the final BC product. The selection of a suitable culture method depends on the final applications of the BC and the desired properties. Other factors such as bacterial strain, oxygen concentration, pH, and nutrition is also an important factor that affects the final BC properties [2]. The most commonly used methods are static method and agitated/shaking method, which detail are given below.

2.4.1 Static method

The static culture method is the simplest and most used culture method for the synthesis of BC materials. In this method, the cultured medium is filled into the vessel and incubated under a static condition with a suitable environment for a certain period of time. The usual condition is 28-30 °C, 4-7 pH, and incubated for 3-14 days. Most of the BC are being produced during trophophase and idiophase of the culture [31]. BC produced by this method are formed in a three-dimensional interconnected reticular shape [32] at the air-liquid interface with increasing thickness of BC as time goes by [2].

On a lab scale, the static culture method is the most used method for the production of BC. However, there are major limitations such as long cultivation time, low productivity rate, and the uneven distribution of the nutrients, oxygen, and bacterial population in the static culture medium [2]. All of these can lead to an uneven formation of BC and result in a BC membrane with irregular thickness [6]. Fed-batch method has also been adopted to increase productivity from the normal batch method.

2.4.2 Agitated/Shaking Method

The agitated culture method has been employed to overcome the major drawbacks of the static method mentioned above. The increased oxygen transfer in agitated culture led to a higher rate of bacterial growth and increased BC production rate. However, excessive mixing can cause BC granules to form in an irregular shape and can also result in insufficient oxygen in the culture medium, which is caused by increasing viscosity in the fermentation broth that can lessen the rate of diffused air into the medium [2]. The less oxygen supply caused the accumulation of other acids such as various acids such as glucuronic acid and acetic acid [21]. This can lower the pH of the broth to below the optimum point, which can trigger the growth of cellulose-negative strains and decrease the production of BC [33]. BC formed in this method are formed in irregular sphere-like shape [2]. The size and shape of the sphere depend on the agitation speed, culture time, and culture medium [34], which can be controlled to obtain BC with desired shape and properties [34].

2.5 Substrate used in the fermentation process

In the cultivation process of BC, a medium called Hestrin and Schramm (HS), which is composed of glucose, yeast extract, peptone, and disodium phosphate is one of the most commonly used substrates for BC fermentation. But HS is not an ideal medium for the process, since by using glucose to act as a sole energy source for the microorganism, gluconic acids are formed, decreasing the pH of the fermentation medium which hinders the growth of BC. Thus, limiting its application in BC production [35]. Furthermore, the use of pure chemicals for carbon sources and vitamin sources in the fermentation process increases the cost of the fermentation medium which accounts for 50-65% [36] of the total production cost, to the point of making the process economically unfeasible for commercial scale production [37].

Thus, finding a cost-effective culture media is important to improve its scale-up capability and decrease its production cost.

Therefore, many alternatives substrate have been used in the past to attempt to lower the cost of BC production by utilizing cheap and easily available substrates for the fermentation process [2]. These low-cost substrates have successfully been utilized for the fermentation process of BC, including fruit juices, which have a large amount of simple sugar, such as glucose, fructose, and sucrose [2], making it an ideal candidate for the alternative substrate to be used in the fermentation process. Other alternative substrates include agricultural waste, industrial waste, and food waste.

2.6 Purification of bacterial cellulose

After the fermentation process, the obtained BC still needs to be purified of the contamination first, because it is still contaminated with the microorganism and other medium components from the process, which can hinder its application [38]. The most commonly used treatments for purifying BC are alkali treatment (NaOH or KOH), organic acid treatment, and repeated washing or a combination of these methods [2]. In alkali treatment, the BC is treated with a NaOH/KOH solution at 80-100 °C for 15-20 minutes to remove entrapped cells, then the BC is repeatedly washed with distilled water to neutralize the pH of the filtrate [2].

2.7 Bacterial cellulose composite synthesis method

Other types of materials can be utilized to increase the properties of BC by incorporating them into the BC structure to create BC composites which can widen its applications. BC has been modified with various methods to achieve various functionality. The modifications include the changing of fiber densities, porosities, crystallinities, chemical structure, and other various properties. The modification method can be grouped into two types, which are an *in-situ* and an *ex-situ* method. The fabrication of conductive BC nanocomposite can be achieved by these two methods.

2.7.1 *In-situ* method

In the *in-situ* method, the materials are added to the medium at the beginning of the fermentation process, this method can change the morphology and physical properties of BC while leaving the chemical composition of the membrane intact [2]. BC produced by this method still contains other impurities such as microorganisms and other medium components from the process and still needs to be purified by the method mentioned above [38]. This method can provide a uniform distribution of the filler materials within the BC with high porosity with excellent mechanical properties with one simple step [39]. Yan, Chen [40] added multi-walled carbon nanotubes (MWCNTs) to the synthetic media and incubated them for two weeks, structural analysis of the BC composite later showed that MWCNTs were trapped between the BC fibrils [40]. This method is the most widely used but has a certain limitation, for example, because of the toxic effect on microorganisms on several important bioactive agents like Ag, ZnO, and TiO_2, these materials cannot be added directly to

the media with the *in-situ* method [11]. BC synthesized with the agitated method cannot be applied as a gel or sheet in biomedical applications, while gel or sheet synthesis with a static method cannot entrap some reinforcement materials for composite synthesis [11].

2.7.2 *Ex-situ* method

On the other hand, in the ex-situ methods, filler materials are incorporated into BC after the synthesis and purification process [11]. First, the fillers and BC microfibers are put into two separate beakers in a suitable solvent at optimum conditions. The filler materials are then dispersed into the BC pellicles by using a homogenizer (mechanical agitation) or with high-energy sonication [41]. The obtained BC with the ex-situ method also requires further purification of residual impurities by washing and drying. The schematic representation of the *in-situ* and *ex-situ* method are shown in Figure 2.

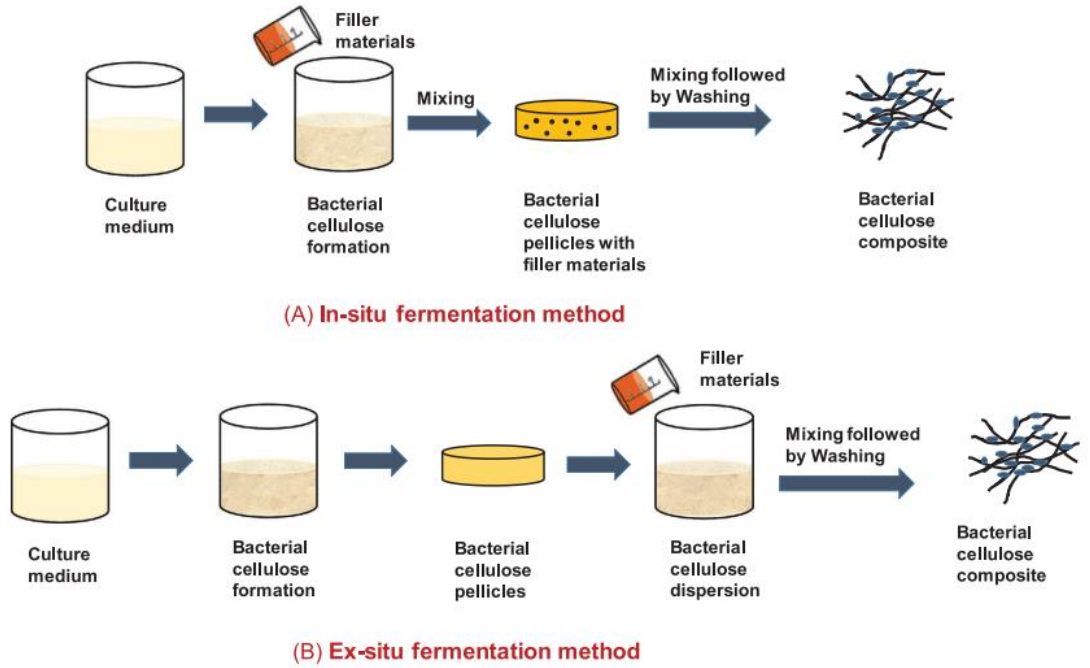

Figure 2. Diagram of BC composite synthesis process by (A) In-situ method and (B) Ex-situ method [2].

2.8 Silver nanoparticles

Silver nanoparticles are tiny particles of silver with sizes ranging from 1 to 100 nanometers. Silver nanoparticles have garnered significant attention due to their small size, large surface area-to-volume ratio, and their exceptional properties, including antibacterial activity, catalytic capabilities, conductivity, and unique optical characteristics [42]. They exhibit strong antimicrobial activity, making them useful in medical devices, wound dressings, and water purification systems [43]. Their catalytic activity enhances chemical reactions, improving efficiency in industrial processes, with excellent electrical conductivity, they are used in electronics and printed circuit

boards [42]. Their optical properties enable advanced sensing and detection in biosensors and environmental monitoring devices [44]. In the field of nanomedicine, silver nanoparticles show promise in drug delivery systems [45]. They also find applications in environmental remediation, solar cells, and photovoltaic devices. The diverse properties of silver nanoparticles make them valuable in various industries and research areas, contributing to advancements in healthcare, electronics, energy, and environmental sustainability.

2.8.1 Methods of silver reduction

The reduction method for synthesizing silver nanoparticles typically involves the use of a reducing agent, which facilitates the conversion of silver ions (Ag^{+}) into silver nanoparticles (Ag^{0}) by providing electrons for the reduction reaction. The most commonly employed method for silver reduction is chemical reduction [46]. Various organic and inorganic reducing agents such as sodium borohydride, sodium citrate, ascorbic acid, and chitosan can be utilized in the reduction of silver ions. Other notable reduction methods include photochemical reduction, thermal reduction, and biological reduction. The choice of a reducing agent and method in the synthesis of silver nanoparticles can significantly impact the resulting particle size. Different reducing agents can influence the reduction kinetics, nucleation process, and growth mechanisms, ultimately affecting the size and size distribution of the nanoparticles [47]. During the reduction process, it is common to employ stabilizing or capping agents, which form a protective layer around the nanoparticles, inhibiting particle-to-particle contact and reducing interparticle attraction, preventing silver nanoparticles from agglomerating [46].

2.9 Bacterial cellulose-silver nanoparticles (BC-Ag) composite

For practical application, silver needs to be integrated into composites or retained inside solid support [18]. For these reasons, BC has been employed as a matrix for synthesizing silver nanoparticles. BC offers several advantages as a matrix; BC contains abundant hydroxyl groups that are capable of reducing Ag^{+} to Ag^{0} [19]. Furthermore, a porous, and interconnected structure provides an ideal matrix for the integration of silver, facilitating uniform dispersion throughout the composite. Additionally, BC could act as both a reducing agent and stabilizing agent in the reduction of silver ions to silver nanoparticles [19], with hydroxyl groups in BC interacting with silver ions and preventing them from agglomerating [19]. This multifunctional role of BC makes it highly advantageous for synthesizing silver nanoparticles and incorporating them into composite materials. The resulting BC-Ag composites exhibit enhanced antimicrobial properties and improved stability, making them suitable for a range of practical applications in areas such as wound healing, biosensors, and antimicrobial coatings. Several research studies [12, 48, 49] have explored various reduction methods to convert silver ions into silver nanoparticles within the BC matrix, with the primary focus being on creating wound-healing materials that can prevent bacterial infections. Schematic depicting the chemical reduction methods for BC-Ag composites are shown in Figure 3

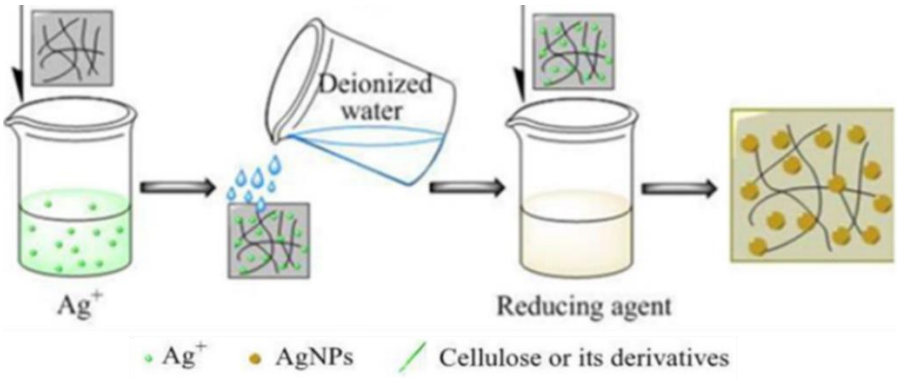

Figure 3. Schematic depicting the chemical reduction methods for BC-Ag composites [50, 51].

CHAPTER THREE: METHODOLOGY AND PROCEDURES

3.1 Materials

The stock culture of *Gluconacetobacter xylinus* bacterial strain AGR 60 was used for BC biosynthesis. Silver nitrate ($AgNO_3$) (purity, >99.8%) was purchased from RCI Labscan Ltd (Bangkok, Thailand). Sucrose and ammonium sulfate were purchased from Ajax Finechem Pty Ltd (New South Wales, Australia). Acetic acid was purchased from Mallinckrodt Chemicals (Paris, KY, USA). Sodium hydroxide (NaOH) pellets were purchased from Kemaus (New South Wales, Australia). Chitosan from shrimp shells with low molecular weight (~25 kDa) was purchased from Marine Bio Resources Co., Ltd. (Samutsakhon, Thailand). Ascorbic acid ($C_6H_8O_6$) was purchased from Loba Chemie Pvt Ltd (Mumbai, India).

3.2 Preparation and purification of BC

BC was prepared by biosynthesis using coconut water as a based substance. Coconut water was mixed with 1.0% acetic acid solution (30%, v/v), 5.0% (w/v) sucrose, and 0.5% (w/v) ammonium sulfate and sterilized at 110 °C for 5 min. Pre-cultures were prepared by a transfer of 15 mL stock culture of *G. xylinus* to 300 mL in 500 mL Erlenmeyer flask and incubated statically at 30 °C for 7 days. Then 5.0% (v/v) of the incubated medium was added to the 75 ml of activated medium and was placed in a glass Petri dish with 14.5 cm diameter and incubated at 30 °C for 7 days.

BC synthesized by the bacteria were harvested at the air-liquid interface of culture broth after 7 days. Then the harvested materials were purified by rinsing them with deionized water (DI) for 30 min, and then immediately placed in 1% (w/v) NaOH solution at room temperature for 24 h to remove attached media and bacterial cells. Then it was washed with running water for 30 min, then rinsed with deionized water (DI) until the pH becomes neutral. Afterward, the purified BC pellicle was stored in DI water at 4°C for subsequent usage. The preparation process diagram of BC is shown in Figure 4.

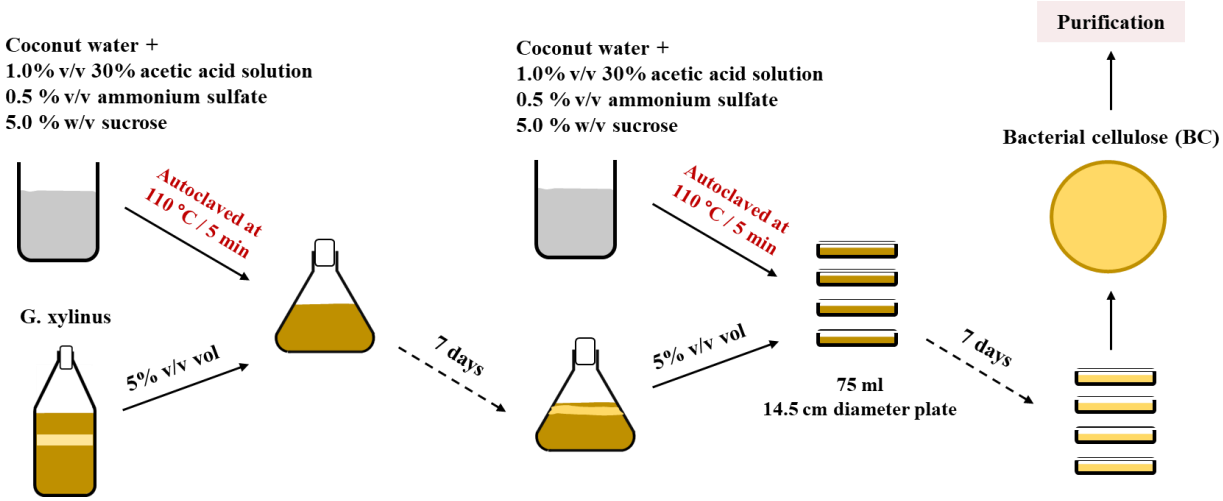

Figure 4. Diagram of the preparation process of BC.

3.3 Impregnation and reduction of Ag ions in BC

BC-Ag composite films were prepared with different methods, some of which were modified from the previous reports. For the reduction of Ag ions by UV irradiation, BC pellicles were pretreated by immersing in 0.02 M $AgNO_3$ solution with constant stirring for 2 h and were left in the dark for 2 days to ensure complete adsorption of Ag ions into the BC matrix. Then, the pretreated BC pellicles were irradiated with UV light (wavelength of 254 nm, 15 W) for 5 h [48, 52].

The chemical reduction was conducted by using ascorbic acid, NaOH, or chitosan. For the reduction of Ag ions using ascorbic acid and NaOH, the pretreated BC pellicles immersed in 0.02 M $AgNO_3$ solution for 2 days were rinsed with DI water to eliminate excess $AgNO_3$ solution. Subsequently, the pellicles of BC-Ag ions were reduced by immersing them in a solution containing 0.12 M ascorbic acid or 0.12 M NaOH for 30 minutes [12, 49]. For the reduction of Ag ions by chitosan, the pellicles of BC were immersed in the solution of 0.02 M $AgNO_3$, 2.0% (w/v) chitosan, and 1.0% (v/v) acetic acid and left in the dark for 2 days. After that, it was incubated at 75 ± 2 °C for 5 h.

After the reduction processes, the pellicles of BC-Ag nanoparticles were then washed with DI water for 10 min to eliminate excess chemicals, then were air-dried at room temperature (30°C) and stored in plastic film at room temperature. The composite films of BC-Ag nanoparticles prepared by reducing silver nitrate using UV irradiation, NaOH, ascorbic acid, and chitosan were denoted as BC-Ag(UV), BC-Ag(NaOH), BC-Ag (Ascorbic), and BC-Ag (Chitosan), respectively. The reduction process diagram is shown in Figure 5.

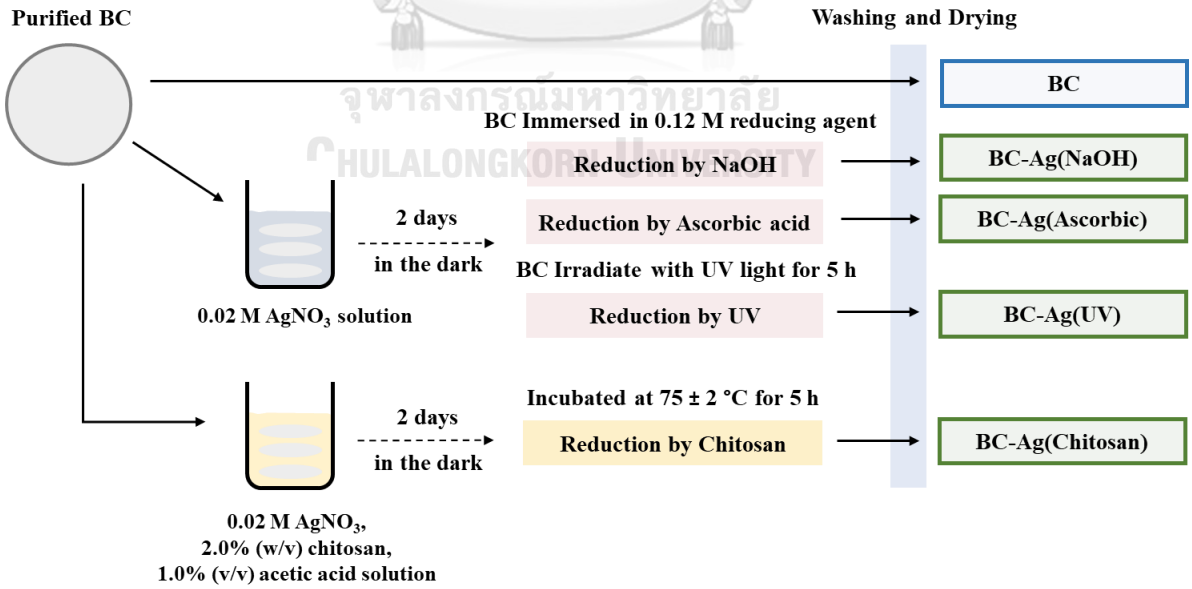

Figure 5. Diagram of the reduction process of BC-Ag composites.

3.4 Physical and Chemical Characterization

The functional groups and chemical structure of BC and BC-Ag composites were determined by Fourier Transform Infrared (FT-IR) Spectroscopy (Spectrum One, Perkin Elmer, Massachusetts, USA) in the ranges of 4000–400 cm^{-1} with a resolution of 4 cm^{-1}.

Morphologies of BC and BC composites were observed by scanning electron microscope and energy dispersive X-ray spectrometer using a Field Emission Scanning Electron Microscopy (FE-SEM, Thermo Fisher Scientific, Quanta 250 FEG, Hillsboro, Oregon, USA). The specimens were sputtered with gold. The SEM–EDS was performed at an accelerating voltage of 5-15 kV.

The mechanical properties of dry films of BC and BC-Ag composites including Young's modulus, tensile strength, and elongation at break, were assessed following the ASTM D882 (2004) standard using a Universal Testing Machine (Hounsfield H10 KM, Redhill, England). The sample were prepared in the form of rectangular film sheets (1×5 cm^2). To ensure repeatability, a minimum of five specimens for each composite type were tested. The test was performed at a temperature of 25 ℃.

The decomposition temperature (T_d) and residual weight were analyzed using a thermogravimetric analyzer (TGA, NETZSCH DSC 204F1, Germany). Film samples weighing between 7–10 mg were subjected to heating from 30 to 600 ℃ under a nitrogen atmosphere, with a constant heating rate of 10 ℃/min.

The glass transition temperature (T_g) of the samples was determined using a differential scanning calorimeter (DSC, NETZSCH TG 209F3, Germany). Approximately 3–6 mg of the sample were loaded into an aluminum pan. The heating process took place under a nitrogen atmosphere, ranging from -100 to 300 ℃, with a constant heating rate of 10 ℃/min.

The crystallinity and structural information of BC and BC-Ag composites were characterized using an X-ray diffractometer (XRD, Bruker AXS Model D8 Discover, Karlsruhe, Germany) with Cu radiation. The measurements were conducted within the 2θ range of 10–80°, with an accelerating voltage of 40 kV and electric current of 40 mA. Crystallinity Index (CI) was calculated using DIFFRAC.EVA software (Version 6.0.0.7) with the following formula.

$$Crystallinity\ (\%) = \frac{Crystalline\ area \times 100}{Total\ Area}$$

Electrical properties of BC and BC-Ag composites were determined by Electrochemical Impedance Spectroscopy (EIS, Squidstat Plus, USA) at 25 ℃, Nyquist plots were obtained using the frequency range from 200 kHz to 1 Hz.

The water absorption capacity (WAC) was evaluated by immersing the weighed dried samples (2×2 cm^2) in DI water at room temperature until they reached

equilibrium. The initial weights of the dry samples were recorded as W_d. After removing the samples from the water and eliminating any excess water on the surface using Kimwipes paper, the weight of each water-swollen sample was then measured, and the weights of the hydrated samples were recorded as W_h. This process was repeated until no further weight change was observed. The WAC was calculated using the following formula.

$$WAC(\%) = \frac{W_h - W_d}{W_d} \times 100$$

3.5 Biological Characterization

The modified JIS Z 2801 method was used to evaluate the antimicrobial properties of composite films against *Staphylococcus aureus* and *Escherichia coli*. To begin, a stock cell suspension of *S. aureus* and *E. Coli* was prepared and allowed to incubate at 37 °C for 16-20 hours. Next, the composite films (3×3 cm^2) were sterilized with UV light for 2 h, then 1 mL of the bacterial cell suspension, with an initial cell density of 1.5-4 × 10^6 CFU/mL, was applied to each swatch. Following a 24 h incubation period at 37 °C, the swatches were subjected to thorough shaking at 200 rpm for 1 minute in the presence of 10 mL of pH 7.4 phosphate-buffered saline (PBS). Subsequently, the PBS solution containing the cells were cultured on agar plates and incubated at 37 °C for another 24 h. Finally, the resulting cell colonies were counted.

CHAPTER FOUR: RESULTS AND DISCUSSION

4.1 Impregnation and *in-situ* reduction of Ag ions

BC is produced from the fermentation process utilizing readily available and cheap coconut water waste as an alternative substrate, which contains nutrient and minerals which plays an important role in microbial growth [53], instead of conventional media like Hestrin and Schramm (HS) medium. To prepare the composites of BC-Ag ions, purified BC pellicles were immersed in $AgNO_3$ solution for two days in the dark for the complete adsorption of Ag^+ into the BC matrix. Abundant hydroxyl groups in BC provide anchoring sites and react with Ag^+ [54]. BC could also act as a stabilizing and a capping agent, as well as a template for the synthesis of AgNPs [55], preventing the agglomeration of AgNPs, which typically occurs in a system lacking capping or stabilizing agent.

After 2-days immersion in the $AgNO_3$ solution, the BC film appeared slightly darker and the $AgNO_3$ solution remained clear. However, under the reduction with chitosan, the BC film that was immersed in $AgNO_3$-chitosan solution became brown and the solution color turned from clear yellow to dark brown. During the incubation at 75 ± 2 °C for 5 h, the colors of the $AgNO_3$-chitosan solution and the composite film were gradually darkening over time. In this case, chitosan also acted as a constituent material in the final composite. For the reduction using the ascorbic acid and NaOH solution, the $AgNO_3$-treated BC film immediately underwent a color change when immersed in the solution of reducing agents. The color of the composite film turned silvery-brown when immersed in the ascorbic acid solution and turned dark brown when immersed in the NaOH solution. Under the reduction using UV light, the composite film gradually turned dark brown when exposed to UV light irradiation. These color changes, consistent with previous cases [48, 49], indicated the reduction of Ag ions to AgNPs, both in the solution and in the composite film.

The reduction mechanisms for each method are as follows. In the reduction by ascorbic acid, ascorbic acid serves as a reducing agent by providing electrons to Ag^+, causing the reduction to Ag^0 and the formation of dehydroascorbic acid [56]. The reduction mechanism of silver ions by NaOH was proposed by Han et al. [57]. They explained that cellulose fiber was capable of reducing Ag^+ to Ag^0 at room temperature under a strong alkali condition. However, Ag^+ ions were unstable under alkaline conditions, resulting in the rapid formation of insoluble Ag_2O particles, which could be reduced by the hydroxyl group of the cellulose, creating another pathway for forming silver nanoparticles. In the UV irradiation method, Ag^+ ions bonded to BC fibers undergo a transformation into silver nanoparticles after being exposed to UV light for a certain period of time, which also resulted in the formation of Ag_2O [48]. In the reduction of silver ions by chitosan, chitosan could act as both a reducing agent and stabilizing agent in the reduction process of Ag^+ ions. The reduction was attributed to the strong coordination abilities and complexation interactions of NH_2

groups with metal ions [58]. Additionally, in this method, chitosan also serves as a filler within the final composites by penetrating the BC matrix, filling the pores, and forming hydrogen bonds with the BC fibrils during the immersion and reduction process [59].

4.2 Morphology

After drying, the colors of BC-Ag films appeared darker. Films of BC-Ag(NaOH), BC-Ag(UV), and BC-Ag(Chitosan) turned from dark brown into black color, while BC-Ag(Ascorbic) films turned into silver color as shown in Figure 6. All BC-Ag films showed a substantial decrease in opacity compared to BC films, ultimately leading to the complete obstruction of light. The thickness of BC, BC-Ag(NaOH), BC-Ag(Ascorbic), BC-Ag(UV), and BC-Ag(Chitosan) films were measured to be 32 ± 3, 51 ± 4, 34 ± 2, 31 ± 3 and 90 ± 10 µm, respectively. Notably, the BC-Ag(Chitosan) films exhibited a considerable increase in thickness, which could be attributed to the diffusion of chitosan into the BC, which formed the intermolecular hydrogen bonds in the BC network [59, 60], resulting in increased thickness of the film. The increased thickness in other BC-Ag films could be attributed to the integration of nanoparticles, particularly Ag_2O in the nanocellulose matrix.

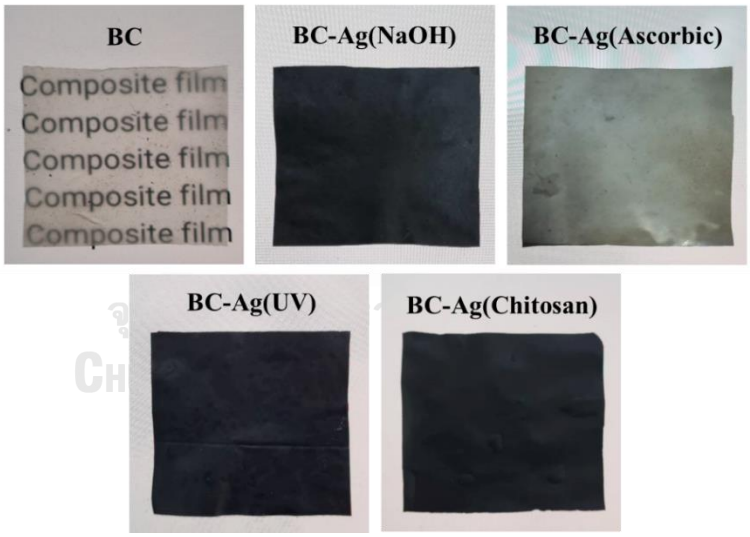

Figure 6. Photographs of dried BC and BC-Ag composites.

FE-SEM analysis was performed on dried BC and BC-Ag composite films, and the observed surface morphology at 50,000× magnification and 5,000× magnification is presented in Figure 7 and Figure 8, respectively. The FE-SEM analysis 50,000× magnification revealed that in all samples, fibers with a consistent diameter can be seen in a mesh-like structure, forming a complex network with different orientations. The fibers exhibit a smooth surface and a cylindrical or ribbon-like shape. The interstitial spaces between the fibers contribute to the porosity of the material, which can be observed as interconnected pores of varying sizes and shapes.

This structure helps silver ions diffuse into the BC structure and distribute evenly inside the material and on the fiber surfaces [48].

Silver nanoparticles with varying diameters can also be seen as white dots on the surface of BC-Ag films. The BC-Ag(Ascorbic) film exhibits the largest diameter of AgNPs, while the BC-Ag(Chitosan) film exhibits the smallest diameter. The smaller size of AgNPs in BC-Ag(Chitosan) can be attributed to the stabilizing or capping capabilities of chitosan on metal nanoparticles [58], which prevents AgNPs from agglomerating and maintaining their smaller sizes. Conversely, the larger size observed in BC-Ag(Ascorbic) could be attributed to the strong reduction ability of ascorbic acid with the lack of stabilizing ability. The size difference of the AgNPs within the BC-Ag composites is of significant importance as it can impact the properties of the materials, such as surface area, reactivity, and its potential applications in fields such as catalysis, sensing, and antimicrobial activities [61-63].

FE-SEM analysis at 5,000× magnification revealed the surface topography of BC and BC-Ag composites. BC-Ag(Ascorbic) and BC-Ag(UV) demonstrated surface topography similar to BC, while BC-Ag(NaOH) surface became rougher, and BC-Ag(Chitosan) surface became noticeably smoother. The smoother surface of BC-Ag(Chitosan) could be attributed to the addition of chitosan within the composite, while the rougher surface of BC-Ag(NaOH) may be attributed to the high amount of silver oxide within the composite. Notably, both composites with observed changes in surface topography, showed an increase in thickness.

EDX scanning is also utilized to determine the chemical composition and the distribution of Ag on the surface of the BC-Ag composites. Figure 9 presents the elemental mapping analysis of Ag and the EDX quantitative analysis of BC-Ag composites at 5,000× magnification. Elemental mapping reveals a uniform distribution of Ag within BC-Ag composites. A prominent peak at around 3 keV from the map sum spectrum analysis confirms the presence of Ag within the materials.

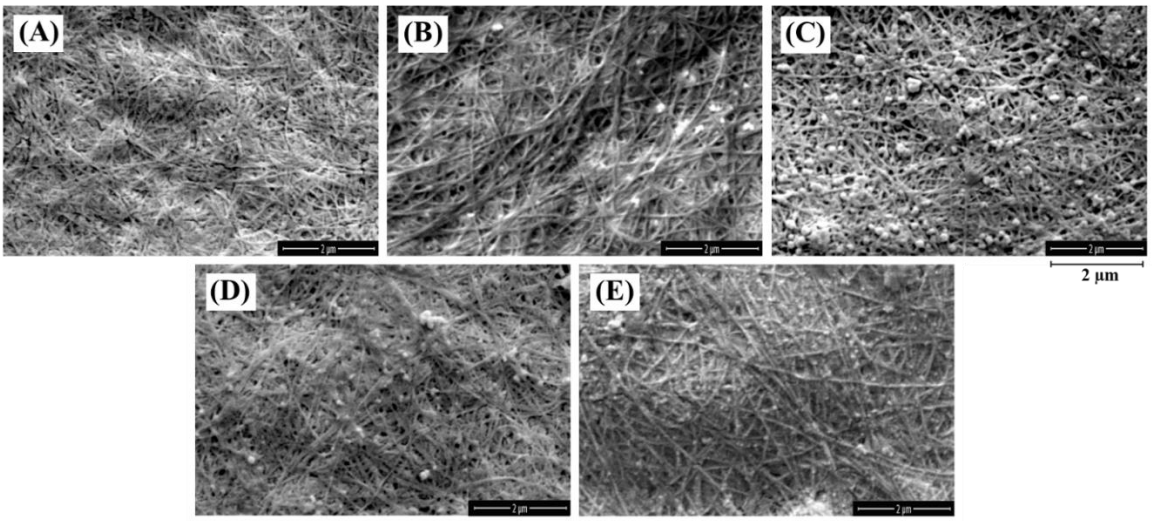

Figure 7. SEM images of dried BC **(A)**, BC-Ag(NaOH) **(B)**, BC-Ag(Ascorbic) **(C)**, BC-Ag(UV) **(D),** and BC-Ag(Chitosan) **(E)** composites at 50,000× magnification.

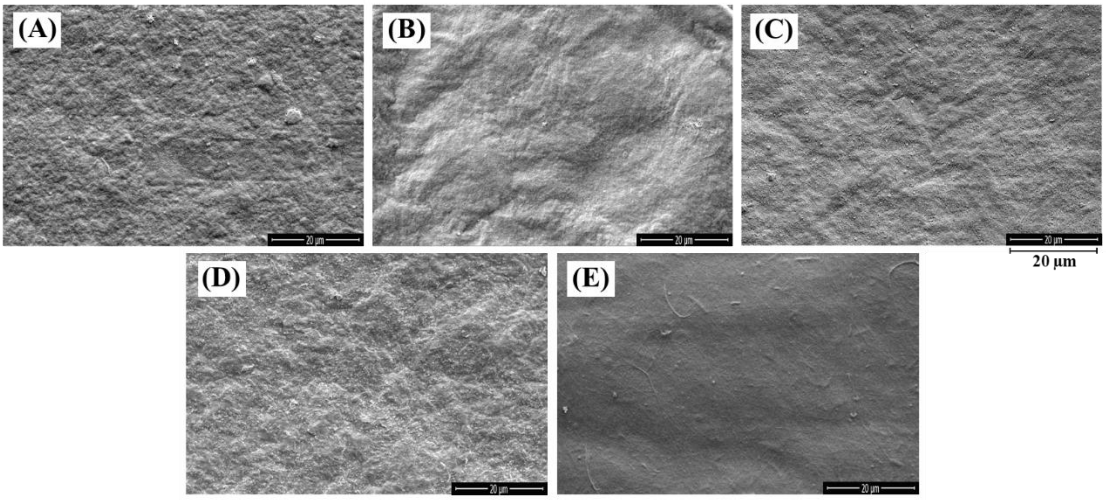

Figure 8. SEM images of dried BC **(A)**, BC-Ag(NaOH) **(B)**, BC-Ag(Ascorbic) **(C)**, BC-Ag(UV) **(D),** and BC-Ag(Chitosan) **(E)** composites at 5,000× magnification.

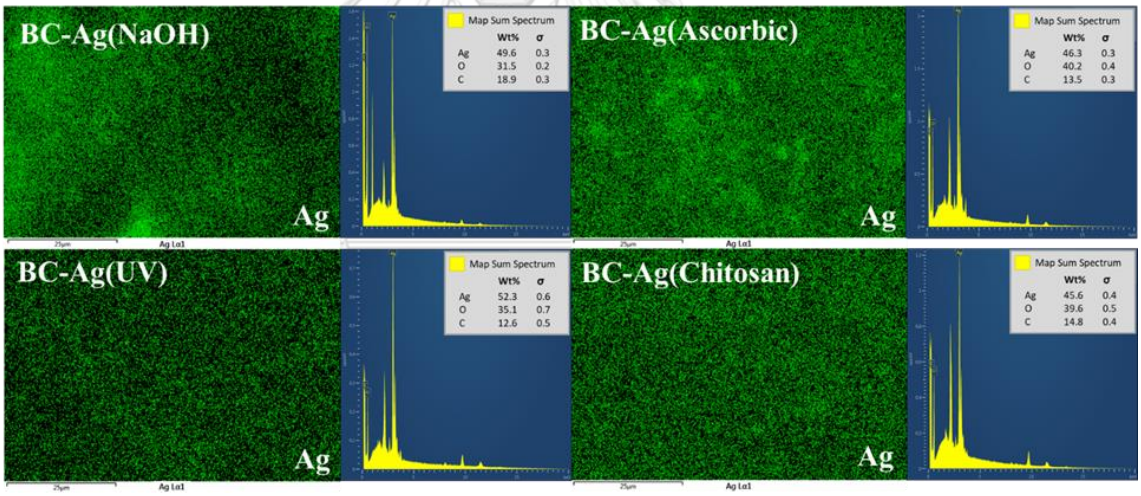

Figure 9. EDX elemental mapping analysis of Ag and map sum spectrum of BC-Ag composites at 5,000× magnification.

4.3 Chemical Interaction

FTIR analysis was performed to investigate the spectra shift. The FTIR spectra of BC and BC-Ag composites are presented in Figure 10. All samples exhibit the characteristic peaks of bacterial cellulose. The first prominent peak is observed as a broad vibration band in the range of 3200-3400 cm^{-1}, indicating the stretching vibration of the abundant O-H groups within the BC network [29]. The peak of BC-Ag shifted very slightly from that of BC film located at 3338 cm^{-1}, which might be caused by AgNPs interfering with the hydrogen bonding of the BC network. The subsequent peaks observed at approximately 2921 cm^{-1} and 2852 cm^{-1} can be

attributed to the asymmetric and symmetric stretching vibration, respectively, of the C-H groups in the cellulose structure [64], these peaks are most prominent in the BC-Ag(UV), BC-Ag(Chitosan) composites. Additionally, both composites exhibit a peak at 1744 cm^{-1}, which could be assigned to non-conjugated C-C stretching [65]. The presence of these three peaks observed in BC-Ag(UV) and BC-Ag(Chitosan) indicated the presence of a capping agent with the AgNPs in the BC structure [65]. The presence of these peaks observed in BC-Ag(UV) and BC-Ag(Chitosan) could be attributed to the capped AgNPs in the BC structure. The intense band between 900-1200 cm^{-1} is attributed to the stretching vibration of the C-O and C-C groups [66]. Furthermore, The band at around 1625 cm^{-1} is assigned to the H-O-H bending of the absorbed water molecules [59] and the band at 1312 cm^{-1} is due to OH in-plane bending [67].

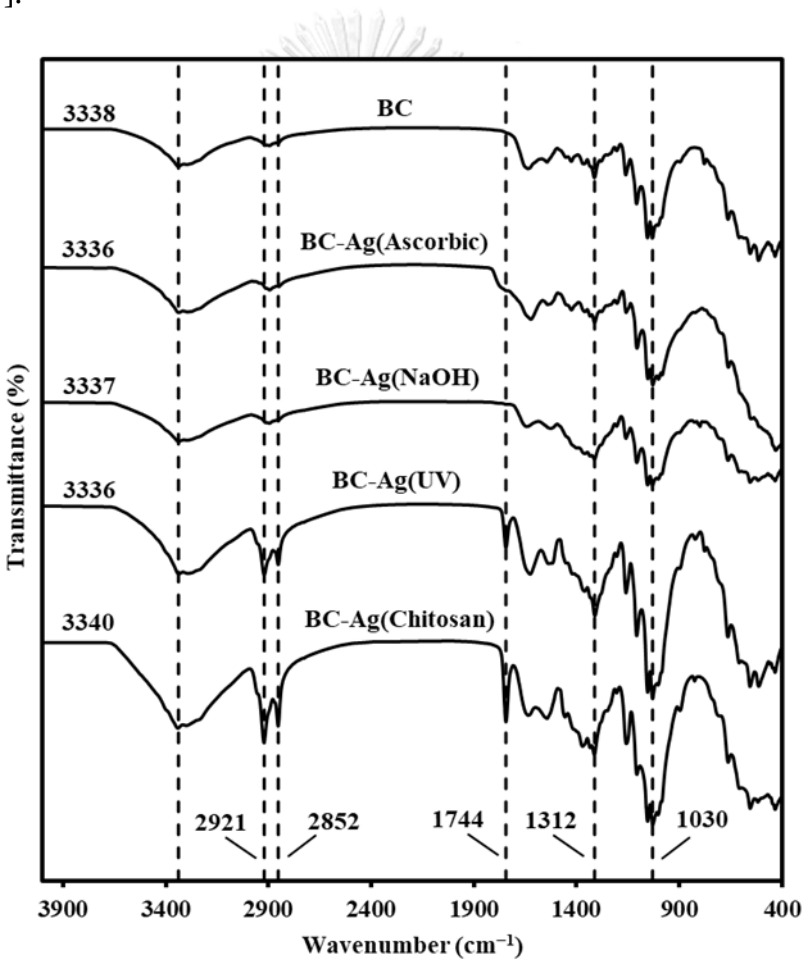

Figure 10. FTIR spectra of BC and BC-Ag composites.

4.4 Crystallinity

The XRD patterns of BC and BC-Ag composites are shown in Figure 11. The XRD diffractograms reveal characteristic peaks of bacterial cellulose in all BC films at 2θ angles of 14.6°, 16.6°, 22.7°, 28.6°, 30.1°, and 46.0°, corresponding to the

crystal surface orientations (101), (110), (002), (130), (122), and (412), respectively, belonging to the crystalline structure of cellulose I (JCPDS No.03-0829) [48, 64, 68]. Additional diffraction peaks at 38.1°, 44.3°. 64.5°, and 77.4° are observed in AgNPs composites, corresponding to the lattice plane values (111), (200), (220), and (311), respectively, of the face-centered cubic metallic silver crystal (JCPDS No.76-1393) [48]. These peaks indicate the presence of AgNPs within the BC network. The other peaks observed at 32.3° for BC-Ag(NaOH), BC-Ag(UV), and BC-Ag(Chitosan) and at 33.7° for BC-Ag(NaOH), are due to the (111) plane of cubic Ag_2O and (100) plane of hexagonal Ag_2O (JCPDS No.72-2108) [69]. Notably, these Ag_2O peaks are absent in BC-Ag(Ascorbic).

Crystallinity Index (CI) was calculated using DIFFRAC.EVA software. The calculated crystallinity index values for BC, BC-Ag(NaOH), BC-Ag(Ascorbic), BC-Ag(UV), and BC-Ag(Chitosan) composites are 78.5%, 68.3%, 83.3%, 69.6%, and 48.6%, respectively. Among BC-Ag composites, the highest degree of crystallinity was observed in BC-Ag(Ascorbic) composites, while BC-Ag(Chitosan) composites showed the lowest degree of crystallinity. Except for BC-Ag(Ascorbic), the incorporation of AgNPs resulted in a slight reduction in the crystallinity of the composites, which could be due to silver interfering with hydrogen bonds within the BC matrix [70]. while chitosan-reduced composites exhibited a significant reduction of crystallinity. The interaction of chitosan molecules with cellulose fibrils might play a significant role in this effect. Previous studies have suggested that the incorporation of a polymer in the BC network can impact the reflection plane of crystalline cellulose, leading to incomplete orientation and decreasing the composite crystallinity [59, 71]. In contrast, the inclusion of AgNPs substantially enhances the crystallinity of the BC-Ag(Ascorbic) composite, possibly due to the interactions between Ag^0 and BC, as well as the absence of Ag_2O which is present in other BC-Ag composites.

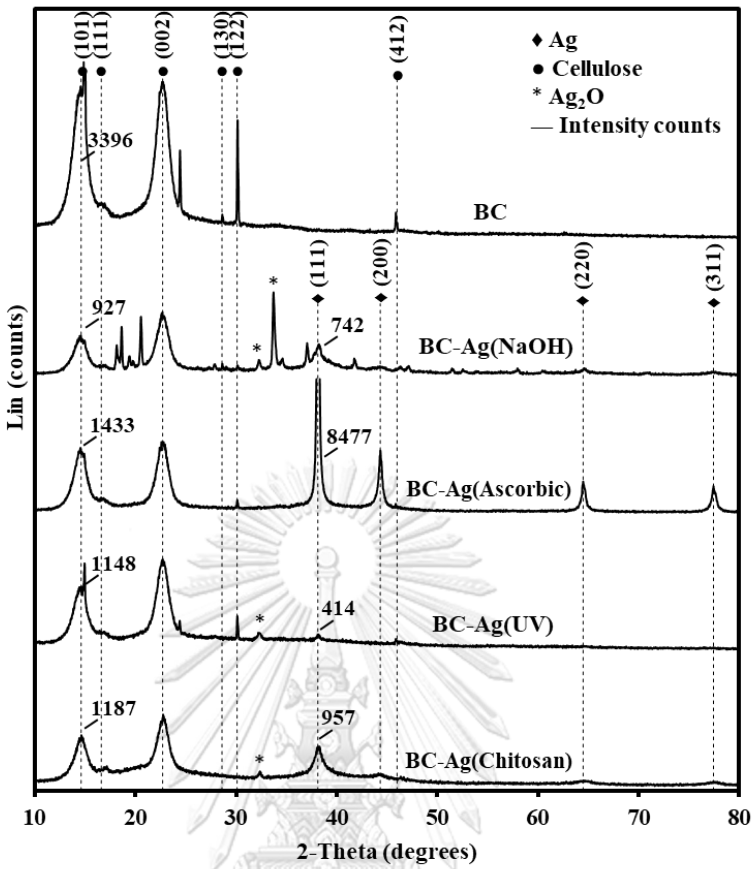

Figure 11. XRD patterns of BC and BC-Ag composites.

4.5 Mechanical Properties

The mechanical properties of BC and BC-Ag composites were investigated using Universal Testing Machine to determine Young's modulus, tensile strength, and elongation at break. The results of the testing are presented in Figure 12. The Young's modulus, tensile strength, and elongation at break of the pristine BC film were measured to be 4945 M7Pa, 165 MPa, and 4.5%, respectively.

The mechanical properties of BC-Ag composites varied greatly by the method of reduction. For BC-Ag(NaOH) and BC-Ag(UV) composites, Young's modulus of the composites dropped dramatically by approximately 50%. Similarly, BC-Ag(Chitosan) exhibited a significant decrease in Young's modulus by about 23%. On the other hand, the composites of BC-Ag(Ascorbic) demonstrated a remarkable increase in Young's modulus, reaching 8960 MPa, which is almost twice the value of pristine BC. These findings are consistent with the crystallinity values obtained from XRD analysis. Except for BC-Ag(Ascorbic), which does not contain Ag_2O, other BC-Ag composites showed lower crystallinity, which might affect mechanical properties. The increase in Young's modulus of BC-Ag(Ascorbic) can be partly attributed to the enhanced crystallinity, which is known to increase Young's modulus in polymers [72].

While BC-Ag(Chitosan) exhibits lower crystallinity than BC-Ag(NaOH) and BC-Ag(UV), its Young's modulus is not affected as much. This is likely due to the presence of chitosan in the composite.

BC-Ag(NaOH) and BC-Ag(UV) composites demonstrated a moderate increase in both tensile strength and elongation at break as compared to BC. Alternatively, BC-Ag(Ascorbic) showed a significant increase in Young's modulus, but elongation at break of the film was decreased by about 60%, while the tensile modulus remained relatively unchanged. The significant decrease in elongation at break for BC-Ag(Ascorbic) could be attributed to the higher rigidity and stiffness of the materials, which resulted from the inclusion of high crystalline silver nanoparticles. In the case of BC-Ag(Chitosan), the presence of chitosan inside the matrix could cause a reduction in flexibility, making the composites noticeably more brittle and resulting in a substantial decrease of approximately 80% in both tensile strength and elongation at break as compared to BC.

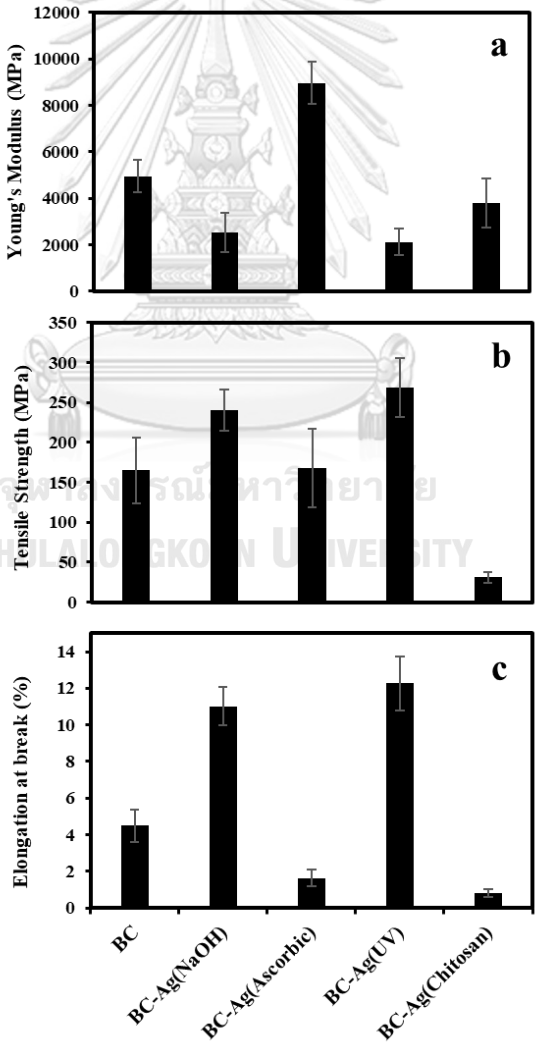

Figure 12. Young's modulus **(a)**, tensile strength **(b)**, and elongation at break **(c)** of BC and BC-Ag composites.

4.6 Thermal Properties

The thermal properties of BC and BC-Ag composites were investigated using differential scanning calorimetry (DSC) (Figure 13a) and thermogravimetric analysis (TGA) (Figure 13b). The TGA curve illustrates the thermal degradation profiles of BC and BC-Ag composites, with the data tabulated in Table 1 and DTG curves illustrates in Figure 14. For pristine BC, the results reveal several stages of thermal degradation. The first stage of minor weight loss occurred between room temperature and 150 °C, which can be attributed to the evaporation of residual water in the BC matrix [73]. The second stage, leading to significant weight loss, occurred between 280 °C and 380 °C, and is attributed to cellulose degradation [74]. For the last stage, a small weight loss is observed between 400 °C and 600 °C, corresponding to the degradation of carbonaceous residues [73, 75]. The degradation profiles of BC-Ag composites were relatively similar to that of BC, with additional weight loss observed around 180 °C to 240 °C for BC-Ag composites, which could potentially be associated with the decomposition of Ag_2O and the capping layers of AgNPs. Additionally, BC-Ag(Chitosan) composite exhibited an additional weight loss at around 240 °C, likely due to chitosan decomposition [76]. The residue mass at 600 °C from TGA analysis can be used to estimate the silver content within the BC-Ag composite, with BC-Ag(NaOH) yielding the highest silver content, while BC-Ag(UV) yields the lowest silver content.

The glass transition temperature (T_g) was measured using DSC thermograms, the obtained T_g data are tabulated in Table 1. The corresponding DSC curves are illustrated in Figure 13a. All samples exhibited an endothermic peak between 90 °C and 98 °C, which relates to the evaporation of water in the BC and BC-Ag composites. Additional endothermic peaks were observed in all BC-Ag composites, which, as mentioned earlier, could be attributed to the decomposition of Ag_2O and the capping layers of AgNPs, as well as the decomposition of chitosan in the case of BC-Ag(Chitosan). The T_g values obtained from DSC were relatively similar across all samples, with BC-Ag composites having slightly lower or similar T_g values compared to BC, except for BC-Ag(Ascorbic), which was 4.8 °C higher than pristine BC. This result is in accordance with crystallinity index (CI) values obtained from XRD analysis, where BC-Ag composites typically exhibit lower CI, except for BC-Ag(Ascorbic).

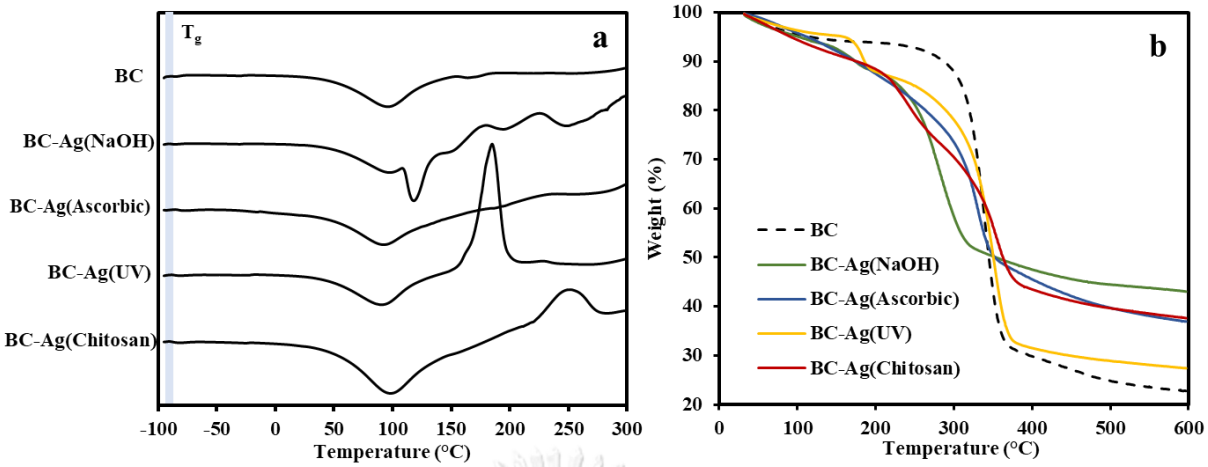

Figure 13. DSC thermograms **(a)** and TGA curves **(b)** of BC and BC-Ag composites.

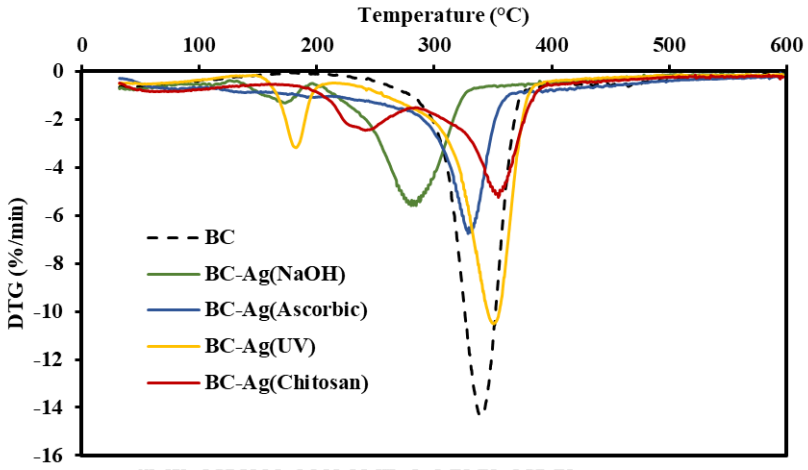

Figure 14. DTG curves of BC and BC-Ag composites.

Table 1. Glass transition temperature (T_g), maximum mass loss rate temperature (T_{max}), % mass loss, and residue at 600 °C of BC and BC-Ag composites.

Samples	Tg (°C)	1st Decomposition		2nd Decomposition		3rd Decomposition		Residue at 600 °C (%)
		T_{max} (°C)	Δ Mass loss (%)	T_{max} (°C)	Δ Mass loss (%)	T_{max} (°C)	Δ Mass loss (%)	
BC	-86.2	44.2	6.2	339.6	64.0	465.2	7.0	22.8
BC-Ag(NaOH)	-87.9	44.2	5.9	172.9	5.6	280.3	45.1	43.0
BC-Ag(Ascorbic)	-81.4	59.3	4.3	328.8	58.7	-	-	36.9
BC-Ag(UV)	-86.1	73.2	4.6	182.5	8.2	350.6	59.8	27.4
BC-Ag(Chitosan)	-86.1	65.5	8.9	241.4	17.6	354.4	35.8	37.6

Note: T_{max} was obtained from derivative thermogravimetric analysis (DTG); T_g was determined using differential scanning calorimetry (DSC) thermograms.

4.7 Electrical Properties

4.7.1 Nyquist plot of BC and BC-Ag composites.

An electrochemical impedance spectroscopy (EIS) study was carried out in a frequency range from 200 kHz to 1 Hz to measure the electrical properties of BC and BC-Ag composites. Figure 15. shows the Nyquist plots of BC and BC-Ag composites. The plots exhibited significant variations depending on the reduction method, with a smaller region of plotted semicircle indicating higher electrical conductivity. The larger semicircle region observed in BC-Ag(Chitosan) compared to pristine BC could be partially attributed to the increased film thickness, resulting in higher electrical resistance. The estimated values of electrical conductivity for BC, BC-Ag(NaOH), BC-Ag(Ascorbic), BC-Ag(UV), and BC-Ag(Chitosan) were calculated from the semicircle region, resulting in calculated conductivities of 2.4×10^{-10}, 1.1×10^{-7}, 5.6×10^{-9}, 1.8×10^{-8}, and 5.8×10^{-10} S/cm, respectively. BC-Ag(NaOH) exhibited the highest conductivity, which was approximately three orders of magnitude higher than pristine BC. The highest conductivity from BC-Ag(NaOH) could be attributed to the high silver content within the matrix. This is supported by the highest residue observed at 600 °C in the TGA analysis (Table 1). While the lowest conductivity of BC-Ag(Chitosan) can be attributed to the non-conductive nature of chitosan within the composites. The presence of double semicircles region in the Nyquist plot of BC-Ag(UV) suggests an uneven distribution of Ag within the composites, which could be due to UV light being unable to reach the inside of the cellulose matrix and only capable of reducing Ag^{+} ions on the outer part.

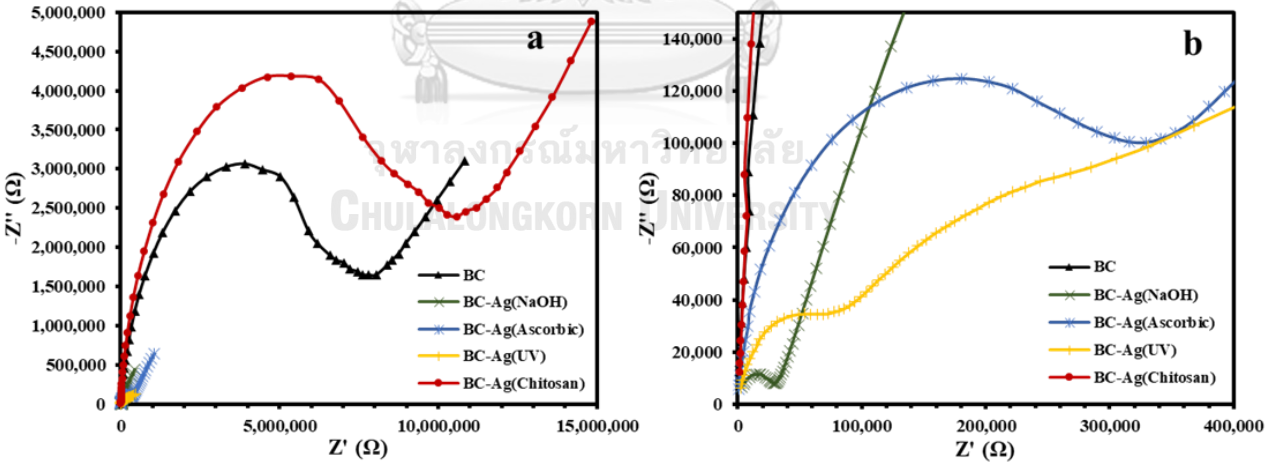

Figure 15. Electrochemical impedance spectroscopy (EIS) spectra (Nyquist plots) with the frequency range from 200 kHz to 1 Hz **(a)** and a magnified view of the high-frequency region of Impedance spectra **(b)** for BC and BC-Ag composites.

4.7.2 Effect of increased Ag concentration for BC-Ag(NaOH)

The effect of increasing Ag concentration on the electrical properties of BC-Ag(NaOH) was further investigated with $AgNO_3$ concentrations of 0.05 M and 0.10

M, compared to the initial concentration of 0.02 M in this study. The NaOH reduction method results in the highest conductivity. However, the increase in $AgNO_3$ concentration did not lead to a significant increase in the conductivity of BC-Ag(NaOH). In addition, the BC-Ag(NaOH) films became increasingly more wrinkled with higher $AgNO_3$ concentration, as depicted in Figure 16. This wrinkling effect could also be observed in SEM images from Figure 8B. This could potentially be attributed to higher aggregation of silver particles at higher concentrations, resulting in the formation of silver cluster. Consequently, this aggregation limited the conductivity and caused greater wrinkling in the films.

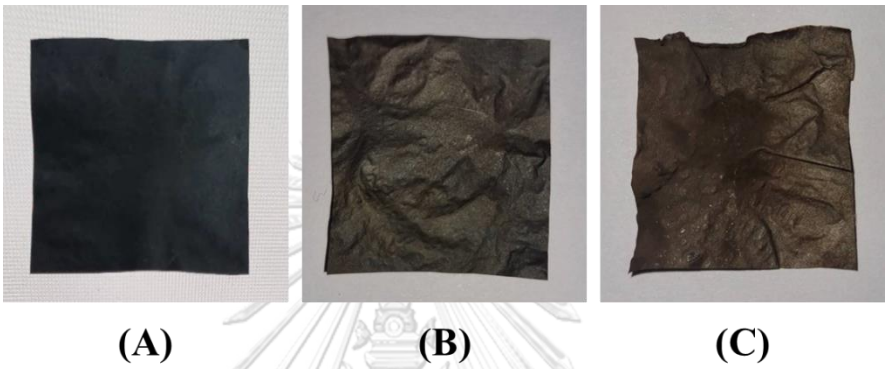

Figure 16. BC-Ag(NaOH) composite impregnated with $AgNO_3$ concentration of 0.02 M **(A)**, 0.05 M **(B)**, and 0.10 M **(C)**.

4.8 Water Absorption Capacity

WAC values of BC and BC-Ag composites were determined using dried films, and the results are illustrated in Figure 17. The WAC of BC, BC-Ag(NaOH), BC-Ag(Ascorbic), BC-Ag(UV), and BC-Ag(Chitosan) composites were 153%, 92%, 66%, 68%, and 344%, respectively. The high WAC of BC can be attributed to its porosity and surface areas. The water molecules are physically trapped both on the surface and within the BC matrix, which is composed of interconnected fibrils [77]. Additionally, hydrogen bonding facilitates the binding of water molecules with the BC fibrils [78].

Besides BC-Ag(Chitosan), the other BC-Ag composites showed lower WAC, which could be attribute to the incorporation of AgNPs into the BC matrix, which made the BC structure denser with lower porosity, thereby reducing water penetration and WAC of the films. The increase in WAC values of BC-Ag(Chitosan) could be attributed to the highly hydrophilic nature of chitosan, which exhibited simultaneous interaction with both water molecules and BC chains [13], resulting in increased absorption of water molecules in the BC matrix, even with a lower pore size and a denser structure as compared to BC [13].

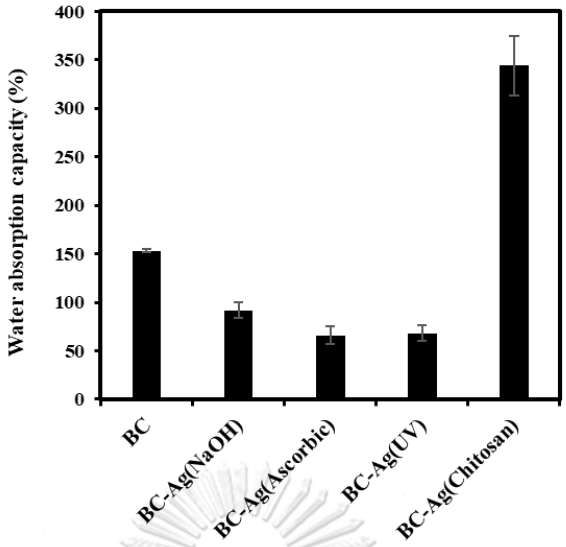

Figure 17. Water absorption capacity (WAC) of BC and BC-Ag composites.

4.9 Antibacterial Activity

BC and BC-Ag composites were tested for antibacterial activities against *S. aureus* and *E. coli*, which served as models of Gram-positive bacteria and Gram-negative bacteria, respectively. The test results are presented in Table 2. For pristine BC, there was a significant increase of 198% and 646% in the viable counts of *S. aureus* and *E. coli*, respectively. In contrast, the growth of *E. coli* and *S. aureus* was strongly inhibited by all types of BC-Ag composites (Reduction of ~10^6 CFU/mL to 0 CFU/ml), to the extent that no visible colonies were observed or detected on the agar plates (Figures 18). These results clearly demonstrated the antibacterial potential of AgNPs and indicate that the antibacterial properties originate from the presence of AgNPs rather than BC. Furthermore, the findings suggest that the antimicrobial effect of BC-Ag composites was not significantly influenced by the method of Ag reduction under the conditions in this study. However, it was previously reported that smaller AgNPs tended to exhibit higher antibacterial activity than larger AgNPs [70], due to the higher total surface area of the nanoparticles [79]. Silver particles were shown to strongly adhere to BC, preventing the leakage of AgNPs from the film [48, 80]. The antibacterial properties of BC-Ag composites can be primarily attributed to their ability to release silver ions (Ag^+) upon contact with moisture [81], which interact with the bacterial cell wall and membrane, disrupting their structure and increasing cell permeability [82].

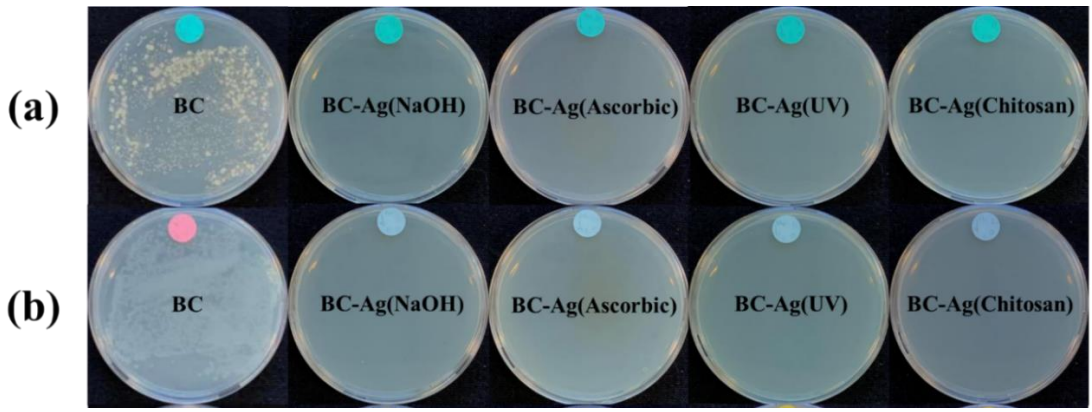

Figure 18. Antibacterial activity of BC and BC-Ag composites against *S. aureus* **(a)** and *E. coli* **(b)** investigated by the plate count method.

Table 2. CFU/mL at 0 h and 24 h contact time intervals with BC and BC-Ag composites against *S. aureus* (A) and *E. coli* (B).

		BC	**BC-Ag (NaOH)**	**BC-Ag (Ascorbic)**	**BC-Ag (UV)**	**BC-Ag (Chitosan)**
(A)	0 h	2.59×10^6	3.21×10^6	3.29×10^6	3.30×10^6	3.23×10^6
	24 h	7.72×10^6	0	0	0	0
	Reduction (Log CFU/ml)	-7.14%	100%	100%	100%	100%
(B)	0 h	1.76×10^6	3.53×10^6	3.55×10^6	3.57×10^6	3.52×10^6
	24 h	1.32×10^7	0	0	0	0
	Reduction (Log CFU/ml)	-13.99%	100%	100%	100%	100%

Note: Negative (-%) values of reduction indicate an increase in viable counts of bacteria.

4.10 Advantages and Disadvantages of Each Reduction Method

Different reduction methods for synthesizing BC-Ag composites have distinct advantages and disadvantages, as summarized in Table 3. NaOH reduction offers high silver content, conductivity, tensile strength, and elongation at break. However, it exhibits a low Young's modulus. Ascorbic acid reduction results in the highest Young's modulus and crystallinity but leads to a larger AgNPs size. UV irradiation reduction requires no chemical reagents, provides high tensile strength and elongation at break, but has the lowest silver content. Chitosan reduction produces AgNPs with the smallest size and highest water absorption capacity, with the addition of chitosan in the composite could potentially enhance antibacterial and wound healing properties due to its ability to release chitosan [59, 83]. However, it exhibits low tensile strength and elongation at break, making it brittle. Lastly, all reduction method exhibits high antibacterial properties.

Table 3. Advantages and disadvantages of each silver reduction method.

Methods of reduction	Advantages	Disadvantages
NaOH reduction	High conductivity High silver content High tensile strength and elongation at break	Low Young's modulus
Ascorbic acid reduction	High Young's modulus High crystallinity	Large AgNPs size
UV irradiation reduction	No chemical reagents required High tensile strength and elongation at break	Low Young's modulus Low silver content
Chitosan reduction	Small AgNPs size High water absorption capacity Enhanced antibacterial and wound healing [59, 83]	Low tensile strength and elongation at break (brittle)

CHAPTER FIVE: CONCLUSIONS AND SUGGESTIONS

5.1 Conclusions

In this work, BC-Ag composites were successfully synthesized using various *in-situ* reduction methods to convert Ag ions to AgNPs, by using sodium hydroxide, ascorbic acid, chitosan, and UV irradiation. The effect of the reduction methods on various properties was investigated. It was observed that AgNPs were effectively attached to BC fibers. BC-Ag(Ascorbic) exhibited the largest size of AgNPs dispersed in the BC matrix, whereas those prepared by using chitosan displayed AgNPs of the smallest size. The result from X-ray diffraction analysis revealed that the incorporation of AgNPs reduced the crystallinity of the composite films, except for the BC-Ag(Ascorbic) which exhibited an increase in crystallinity. The mechanical properties of the BC-Ag composites varied greatly depending on the reduction methods. BC-Ag(Ascorbic) showed a remarkable increase in Young's modulus. The composites of BC-Ag(NaOH) and BC-Ag(UV) showed a significant increase in tensile strength and elongation at break; whereas, the BC-Ag(Chitosan) composite became brittle and exhibited a significant decrease in tensile strength and elongation at break. Thermal analysis indicated that the decomposition profiles and T_g of the composites were quite similar to BC; only a small increase in T_g was noticed for BC-Ag(Ascorbic). Additional weight loss steps were observed for BC-Ag composites at high temperatures during TGA analysis. Electrochemical Impedance Spectroscopy analysis demonstrated that BC-Ag(NaOH) exhibited the highest conductivity at 1.1×10^{-7} S/cm, which was approximately three orders of magnitude higher than pristine BC, while the conductivity of the other BC-Ag composites, except for BC-Ag(Chitosan), increased to some extent. The WACs of BC-Ag composites tended to decrease by the incorporation of AgNPs; however, the WAC of BC-Ag(Chitosan) increased owing to the presence of chitosan within the BC matrix. Antibacterial tests showed that all BC-Ag composites possessed a very strong inhibitory effect against *E. coli* and *S. aureus*. These multifaceted properties of BC-Ag composites highlight their potential applications in various fields such as antimicrobial packing, wound dressings, and biomedical devices. These findings should contribute to a better understanding of the BC-Ag composites and open avenues for further exploration and optimization of their properties for specific applications.

5.2 Suggestions

Variations in concentrations of reduction agents, concentrations of silver, and reduction procedure should be tested further to assess their influence on the properties of the final Ag composites and additional research should be conducted to investigate the antibacterial activity at lower concentrations of $AgNO_3$, to determine the impact of the reduction method and find the optimum concentration of silver on the antibacterial properties. Additional transmission electron microscopy (TEM) analysis could also be conducted to determine the shape and size of silver nanoparticles.

APPENDIX

APPENDIX A. SEM images with the original scale bar

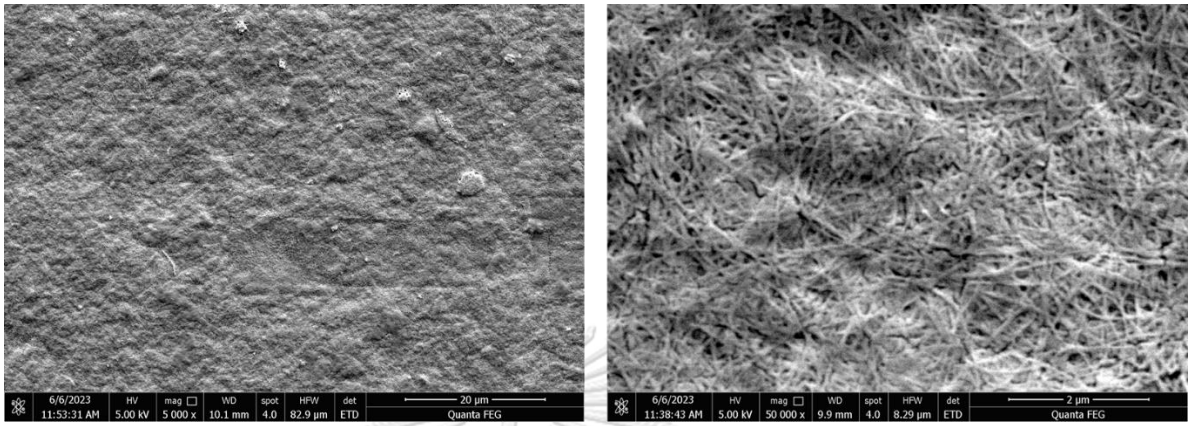

Figure 19. SEM images of BC at 5,000× magnification (left) and 50,000× magnification (right) magnification.

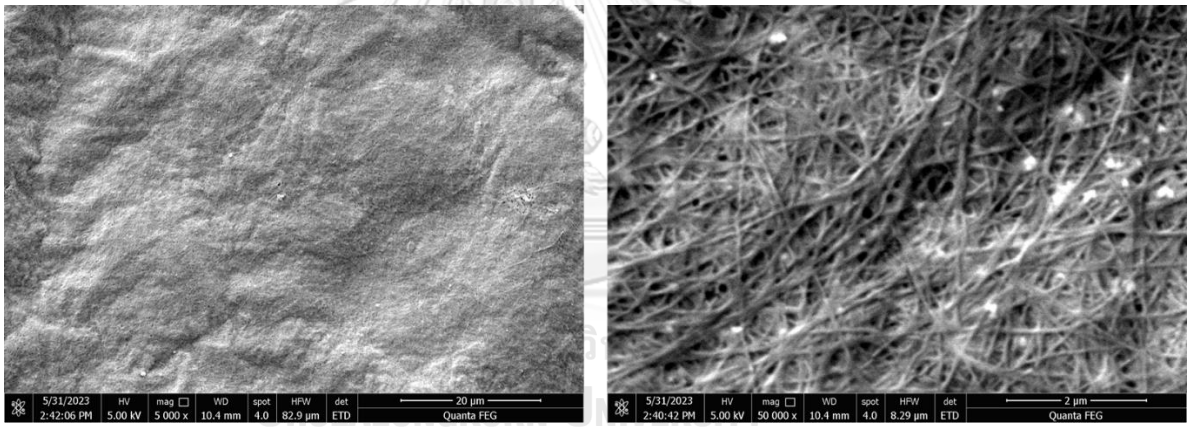

Figure 20. SEM images of BC-Ag(NaOH) composite at 5,000× magnification (left) and 50,000× magnification (right) magnification.

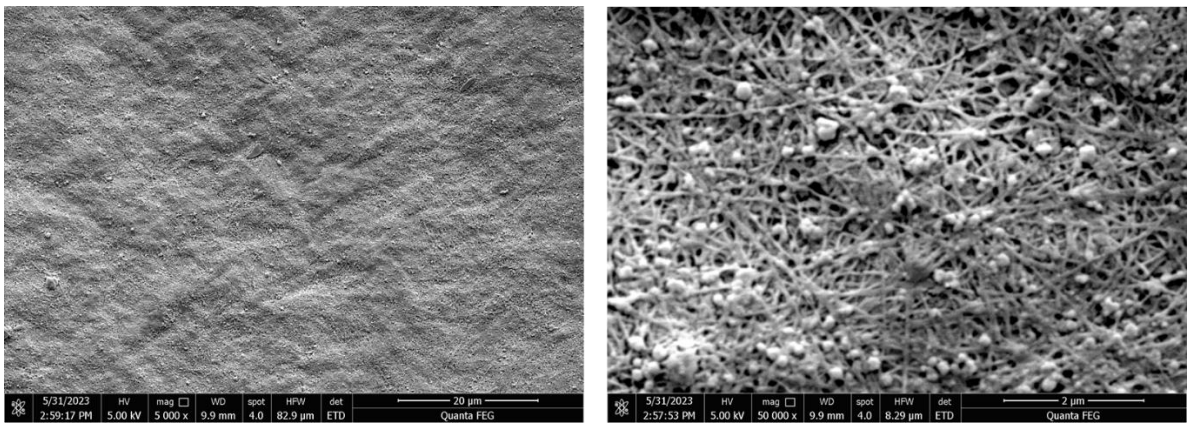

Figure 21. SEM images of BC-Ag(Ascorbic) composite at 5,000× magnification (left) and 50,000× magnification (right) magnification.

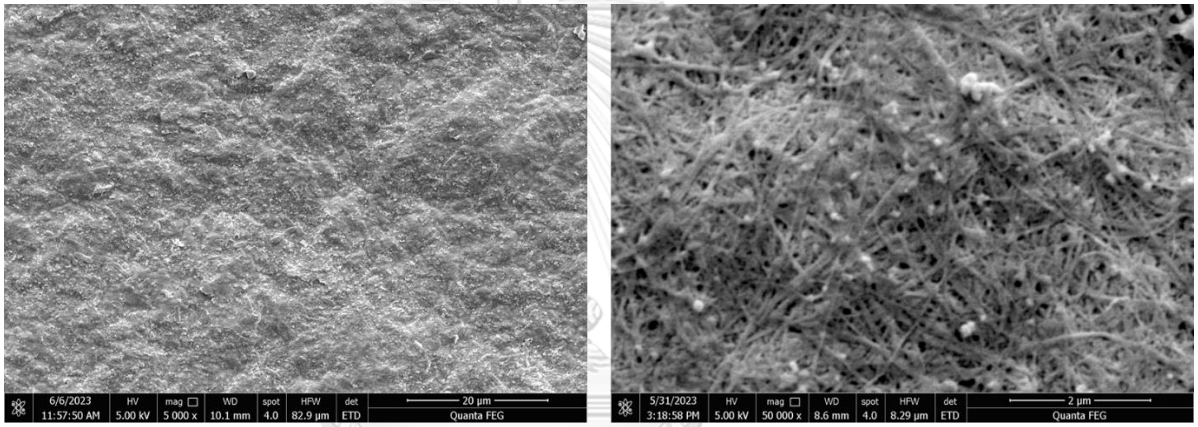

Figure 22. SEM images of BC-Ag(UV) composite at 5,000× magnification (left) and 50,000× magnification (right) magnification.

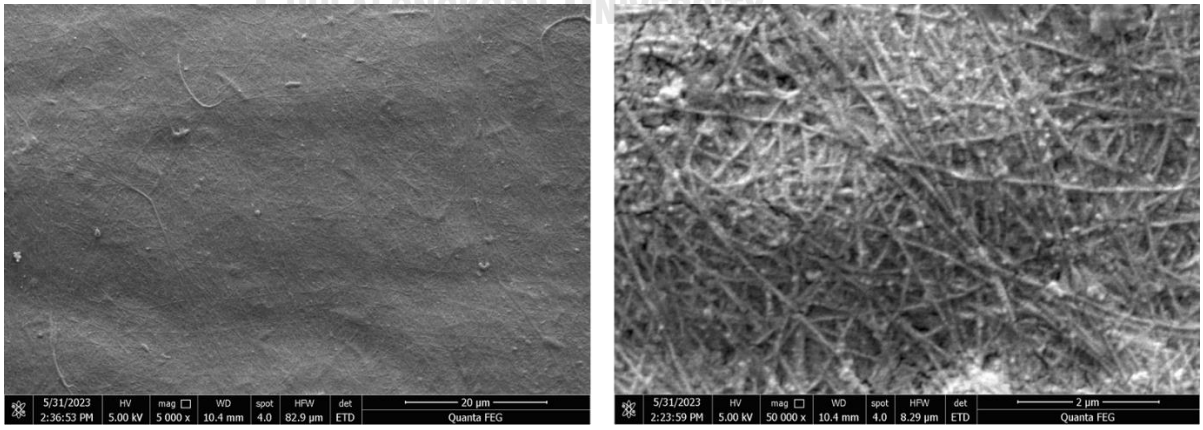

Figure 23. SEM images of BC-Ag(Chitosan) composite at 5,000× magnification (left) and 50,000× magnification (right) magnification.

APPENDIX B. Peak analysis data for XRD

Table 4. Peak analysis data for XRD peaks for BC.

Angle (2-theta)	d value (angstrom)	Intensity Counts	Relative Intensity
14.561	6.0784	3396	31.60%
14.9804	5.9092	9694	100.00%
16.6338	5.3254	840	3.40%
22.7306	3.9089	3520	32.50%
24.4204	3.6421	1959	15.80%
28.621	3.1164	581	1.90%
30.1404	2.9627	2646	24.70%
30.7954	2.9011	413	0.50%
34.3468	2.6088	387	0.80%
45.8802	1.9763	615	4.40%
46.3399	1.9578	268	0.60%
50.0016	1.8226	225	0.60%
62.6008	1.4827	214	0.70%

Table 5. Peak analysis data for XRD peaks for BC-Ag(NaOH).

Angle (2-theta)	d value (angstrom)	Intensity Counts	Relative Intensity
14.4603	6.1205	927	44.80%
16.8796	5.2483	311	6.20%
18.1366	4.8873	727	30.70%
18.3002	4.844	478	15.70%
18.6203	4.7614	1136	55.10%
19.4	4.5718	503	16.90%
19.7409	4.4936	405	10.90%
20.5387	4.3208	1371	68.80%
22.676	3.9182	1433	72.50%
26.1814	3.401	263	3.10%
27.3134	3.2625	262	3.40%
27.8822	3.1973	330	7.50%
28.6214	3.1163	335	8.00%
29.0425	3.0721	261	3.70%
30.1195	2.9647	298	6.30%
30.3754	2.9403	241	3.00%
32.3191	2.7677	412	12.60%
33.7187	2.656	1880	100.00%
34.6198	2.5889	447	13.60%
37.0601	2.4238	768	32.20%
37.8199	2.3769	581	21.00%
38.1634	2.3563	742	30.60%
39.2673	2.2925	406	10.50%
40.2207	2.2404	326	5.90%

Angle (2-theta)	d value (angstrom)	Intensity Counts	Relative Intensity
41.4816	2.1751	290	4.00%
41.7393	2.1623	441	13.20%
44.3009	2.043	277	4.60%
45.8423	1.9778	224	2.50%
46.3627	1.9569	276	6.00%
47.1573	1.9257	278	6.80%
51.4411	1.775	230	5.90%
52.5407	1.7404	214	4.80%
54.0809	1.6944	166	2.00%
57.9714	1.5896	239	6.80%
60.4261	1.5308	179	3.40%
64.567	1.4422	230	6.10%
70.8168	1.3295	143	2.40%
77.28	1.2336	158	3.60%

Table 6. Peak analysis data for XRD peaks for BC-Ag(Ascorbic).

Angle (2-theta)	d value (angstrom)	Intensity Counts	Relative Intensity
14.5312	6.0908	1479	15.60%
16.5803	5.3424	408	2.30%
16.8217	5.2663	382	2.00%
22.7014	3.9139	1615	16.90%
30.1105	2.9655	348	2.20%
34.3759	2.6067	242	0.60%
36.1831	2.4805	282	0.90%
38.1322	2.3581	8447	100.00%
44.3395	2.0413	1408	14.80%
45.8453	1.9777	256	1.00%
64.4875	1.4438	740	7.70%
77.4403	1.2315	640	6.60%

Table 7. Peak analysis data for XRD peaks for BC-Ag(UV).

Angle (2-theta)	d value (angstrom)	Intensity Counts	Relative Intensity
14.5161	6.0971	1448	68.30%
14.9409	5.9247	1937	96.80%
16.8422	5.2599	475	9.80%
22.7026	3.9137	2036	100.00%
24.3997	3.6451	705	21.70%
27.9204	3.193	386	3.70%
30.1205	2.9646	814	29.80%
32.2824	2.7708	447	9.00%
38.1277	2.3584	414	8.20%

Angle (2-theta)	d value (angstrom)	Intensity Counts	Relative Intensity
45.8602	1.9771	306	5.80%
46.2004	1.9633	266	3.60%
64.6369	1.4408	164	1.50%

Table 8. Peak analysis data for XRD peaks for BC-Ag(Chitosan).

Angle (2-theta)	d value (angstrom)	Intensity Counts	Relative Intensity
14.63	6.0499	1187	69.60%
16.3831	5.4063	474	8.70%
16.8407	5.2604	506	10.60%
17.1621	5.1626	525	11.70%
18.254	4.8562	453	4.60%
22.7514	3.9054	1648	100.00%
32.3787	2.7628	413	11.10%
38.1391	2.3577	957	50.70%
44.1422	2.05	369	6.90%
46.3602	1.957	285	4.00%
64.5439	1.4427	227	5.90%
77.4392	1.2315	191	4.90%

APPENDIX C. The calculation of the conductivity value

Conductivity values were calculated using:

$$\sigma = \frac{1}{Z}\left(\frac{L}{A}\right)$$

Where; σ = Conductivity (S/cm)

Z = Complex impedance (ohms)

L = Length of the conductor (cm)

A = Cross-sectional area (cm^2)

With Z calculated from

$$|Z|^2 = |Z'|^2 + |Z''|^2$$

Where; Z' = Real part of the complex impedance (ohms)

Z" = Imaginary part of the complex impedance (ohms)

APPENDIX D. Antibacterial assessment plate count results

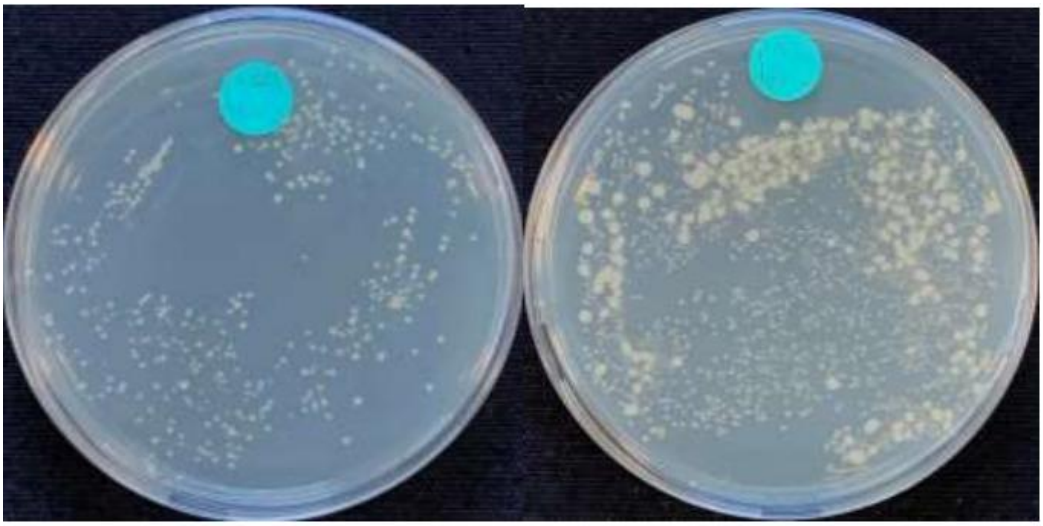

Figure 24. The number of bacteria *Staphylococcus aureus* on BC sample at time 0 day at dilution 10^{-3} (A), 1 day at dilution 10^{-3} (B).

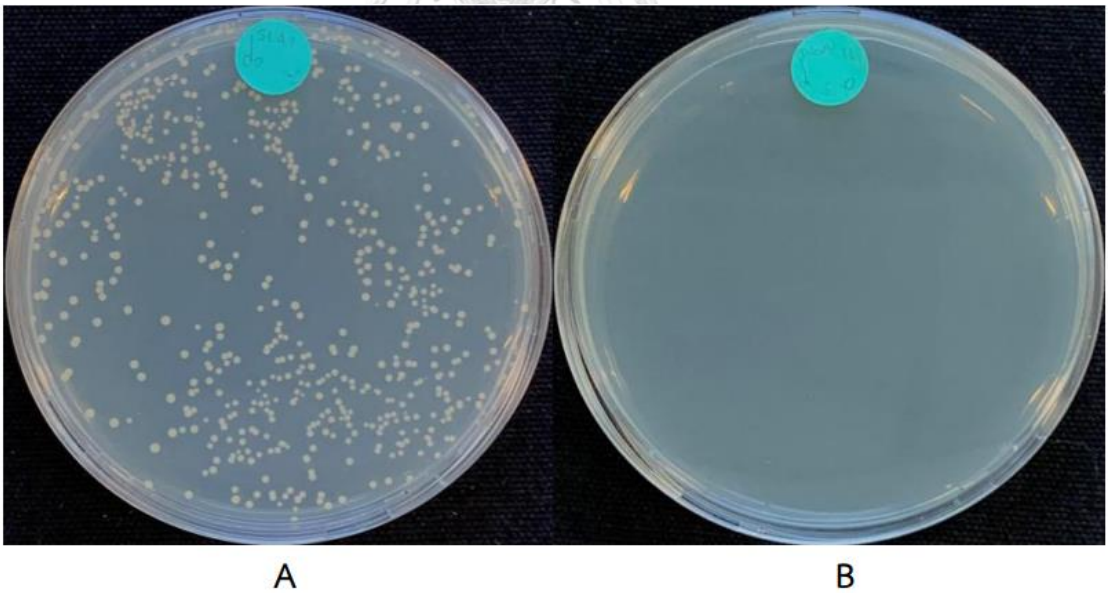

Figure 25. The number of bacteria *Staphylococcus aureus* on BC-Ag(NaOH) sample at time 0 day at dilution 10^{-3} (A), 1 day at dilution 10^{0} (B).

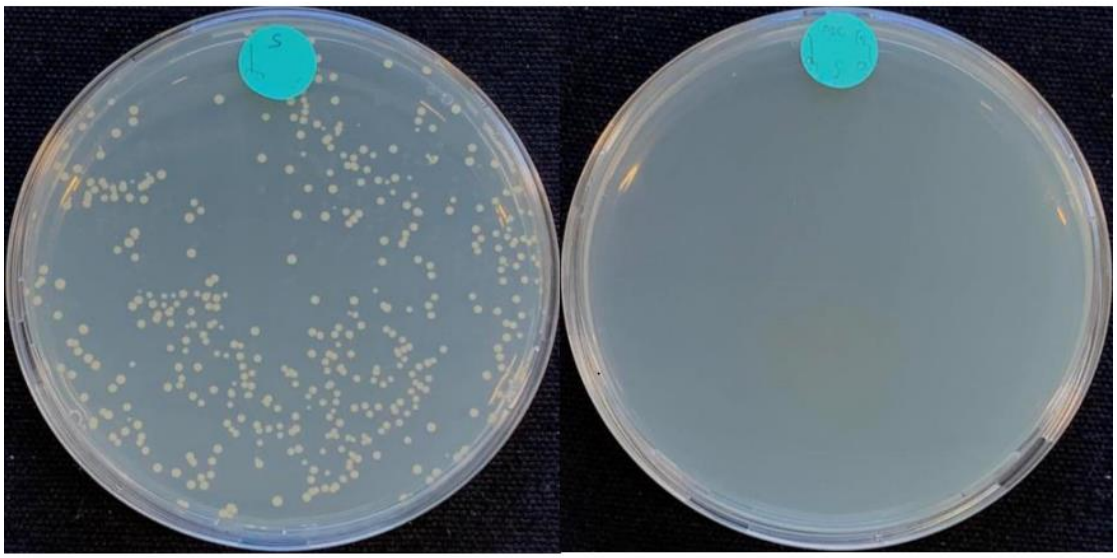

A B

Figure 26. The number of bacteria *Staphylococcus aureus* on BC-Ag(Ascorbic) sample at time 0 day at dilution 10^{-3} (A), 1 day at dilution 10^{0} (B).

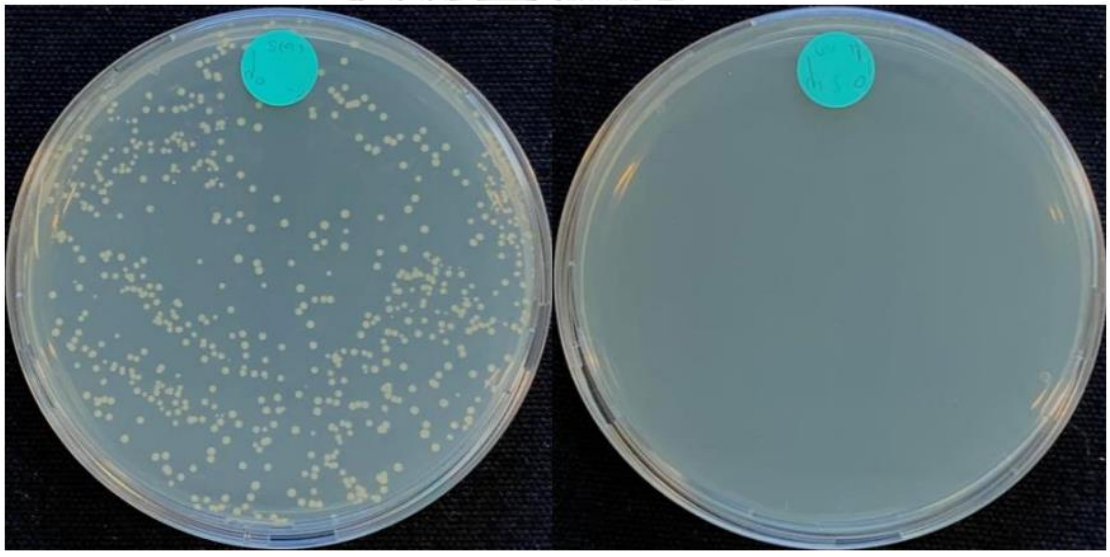

A B

Figure 27. The number of bacteria *Staphylococcus aureus* on BC-Ag(UV) sample at time 0 day at dilution 10^{-3} (A), 1 day at dilution 10^{0} (B).

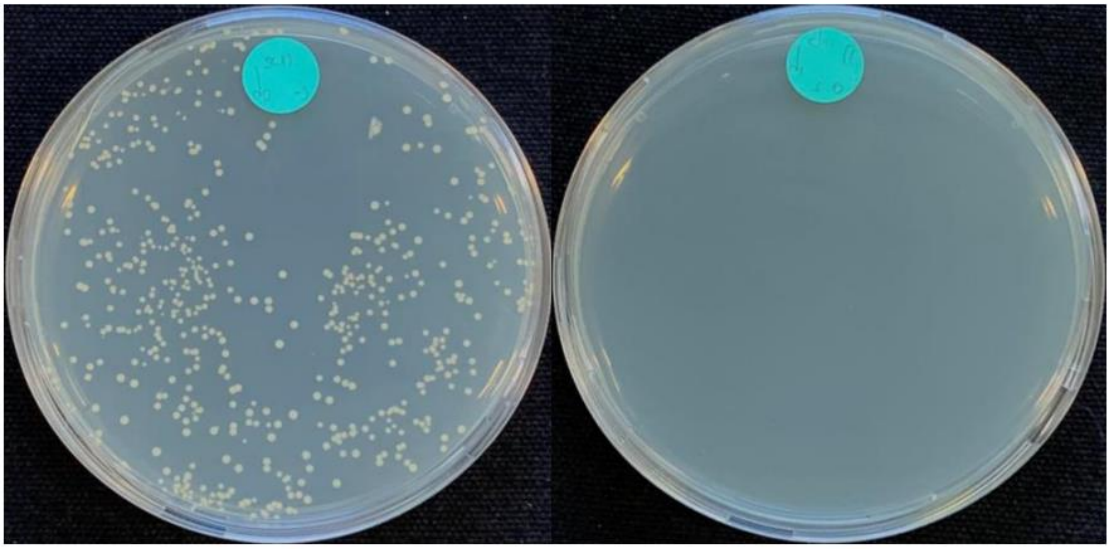

Figure 28. The number of bacteria Staphylococcus aureus on BC-Ag(Chitosan) sample at time 0 day at dilution 10^{-3} (A), 1 day at dilution 10^{0} (B).

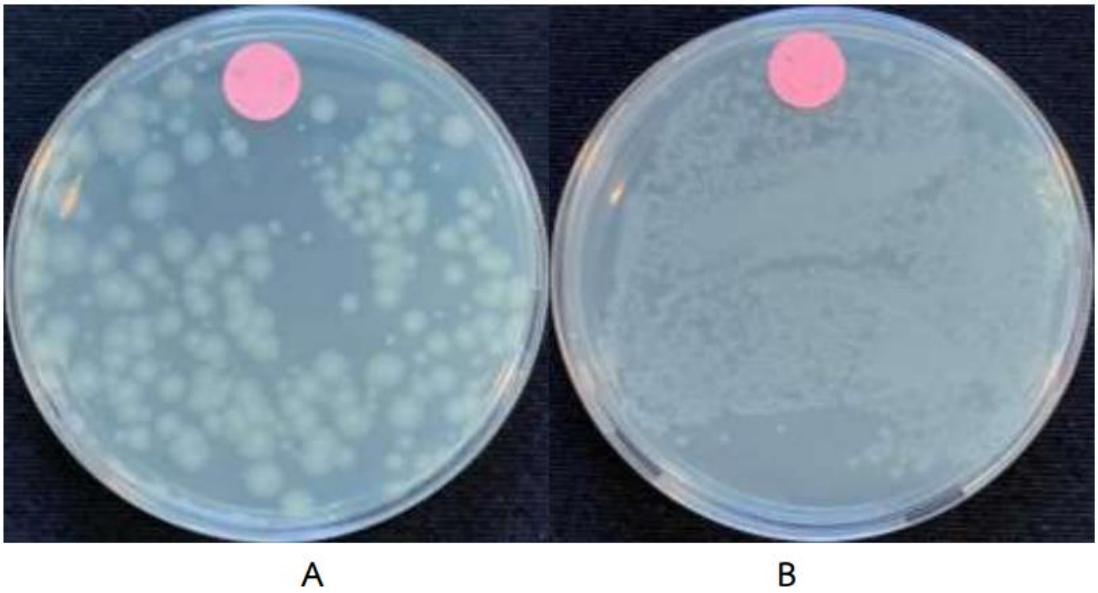

Figure 29. The number of bacteria *Escherichia coli* on BC sample at time 0 day at dilution 10^{-3} (A), 1 day at dilution 10^{-3} (B).

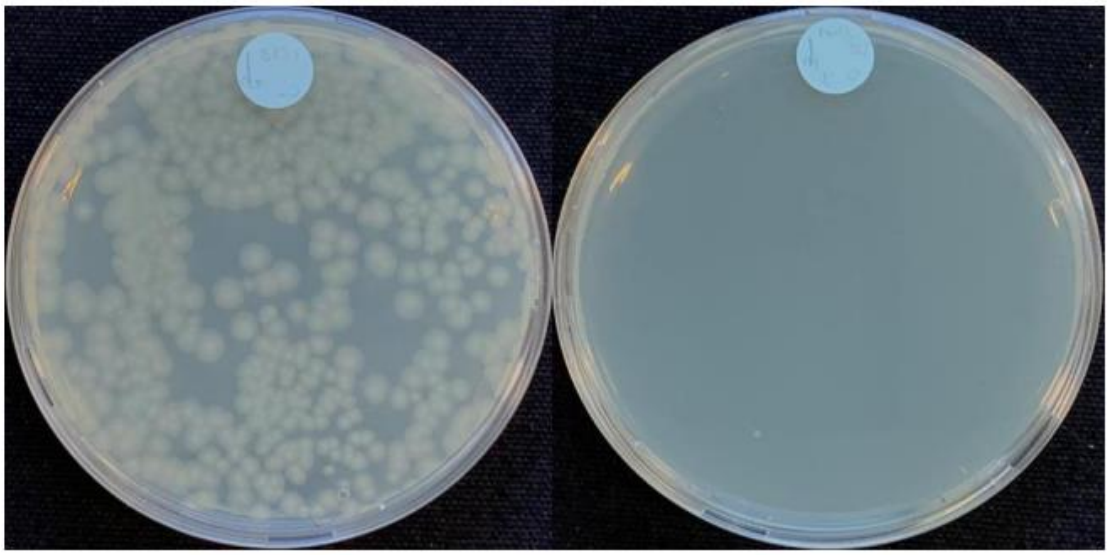

Figure 30. The number of bacteria *Escherichia coli* on BC-Ag (NaOH) sample at time 0 day at dilution 10^{-3} (A), 1 day at dilution 10^{0} (B).

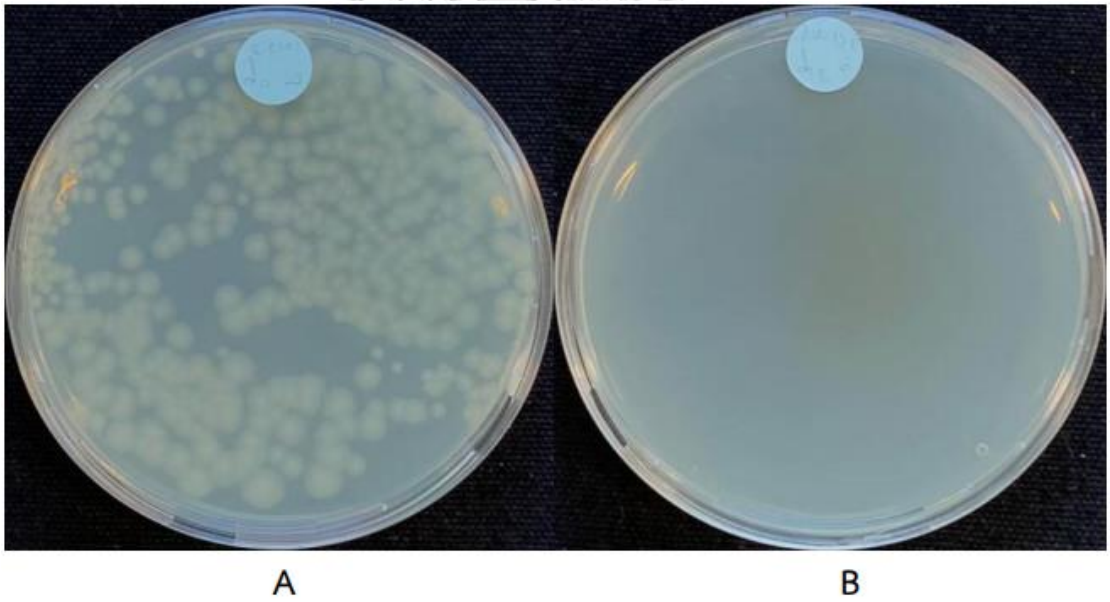

Figure 31. The number of bacteria Escherichia coli on BC-Ag (Ascorbic) sample at time 0 day at dilution 10^{-3} (A), 1 day at dilution 10^{0} (B).

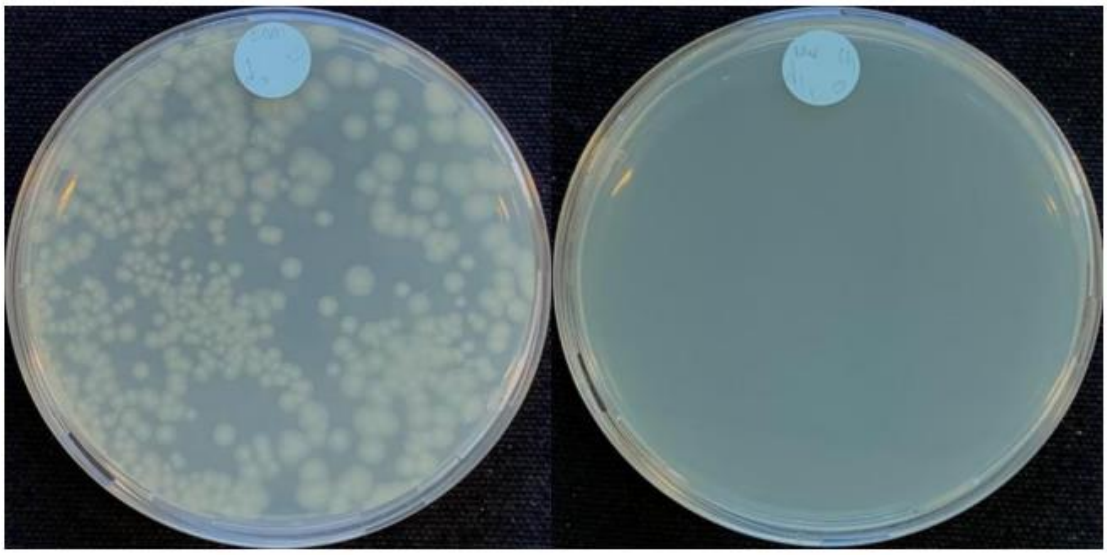

Figure 32. The number of bacteria Escherichia coli on BC-Ag(UV) sample at time 0 day at dilution 10^{-3} (A), 1 day at dilution 10^{0} (B).

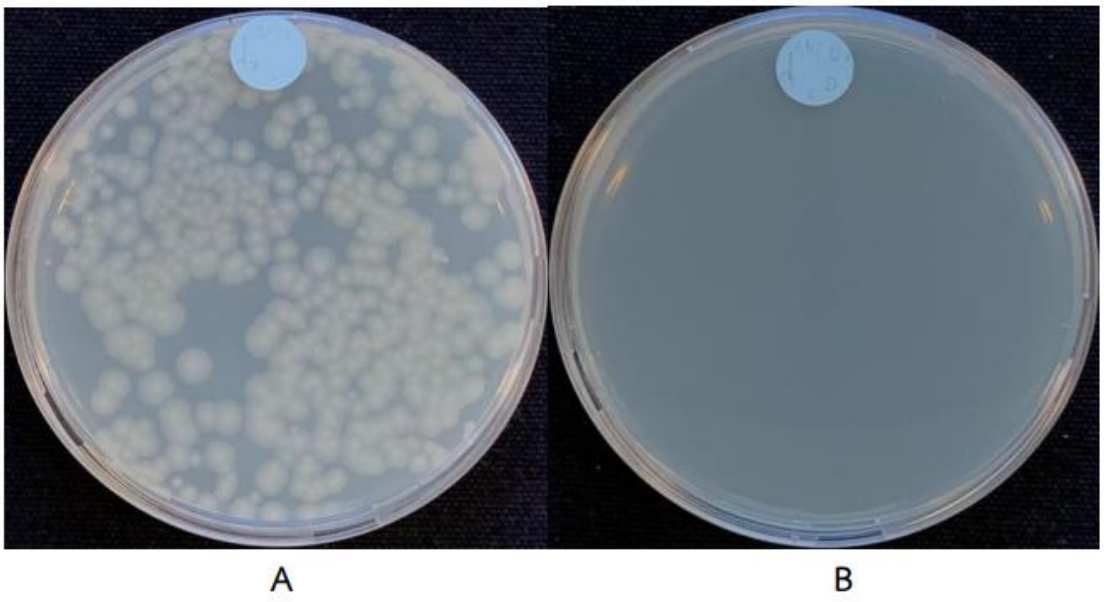

Figure 33. The number of bacteria *Escherichia coli* on BC-Ag(Chitosan) sample at time 0 day at dilution 10^{-3} (A), 1 day at dilution 10^{0} (B).

REFERENCES

1. Habibi, Y., L.A. Lucia, and O.J. Rojas, *Cellulose nanocrystals: chemistry, self-assembly, and applications.* Chemical reviews, 2010. **110**(6): p. 3479-3500.
2. Poddar, M.K. and P.K. Dikshit, *Recent development in bacterial cellulose production and synthesis of cellulose based conductive polymer nanocomposites.* Nano Select, 2021. **2**(9): p. 1605-1628.
3. Sintharm, P. and M. Phisalaphong, *Green Natural Rubber Composites Reinforced with Black/White Rice Husk Ashes: Effects of Reinforcing Agent on Film's Mechanical and Dielectric Properties.* Polymers, 2021. **13**(6): p. 882.
4. Supanakorn, G., et al., *Alginate as Dispersing Agent for Compounding Natural Rubber with High Loading Microfibrillated Cellulose.* Polymers, 2021. **13**(3): p. 468.
5. Dikshit, P.K. and B.S. Kim, *Bacterial cellulose production from biodiesel–derived crude glycerol, magnetic functionalization, and its application as carrier for lipase immobilization.* International journal of biological macromolecules, 2020. **153**: p. 902-911.
6. Blanco Parte, F.G., et al., *Current progress on the production, modification, and applications of bacterial cellulose.* Crit Rev Biotechnol, 2020. **40**(3): p. 397-414.
7. Ciechańska, D., *Multifunctional bacterial cellulose/chitosan composite materials for medical applications.* Fibres and Textiles in Eastern Europe, 2004. **12**: p. 69-72.
8. Evans, B.R., et al., *Palladium-bacterial cellulose membranes for fuel cells.* Biosensors & bioelectronics, 2003. **18 7**: p. 917-23.
9. Choi, Y.-J., et al., *Preparation and characterization of acrylic acid-treated bacterial cellulose cation-exchange membrane.* Journal of Chemical Technology and Biotechnology, 2004. **79**: p. 79-84.
10. Jeon, J.-H., et al., *Bacterial cellulose actuator with electrically driven bending deformation in hydrated condition.* Sensors and Actuators B: Chemical, 2010. **146**(1): p. 307-313.
11. Shah, N., et al., *Overview of bacterial cellulose composites: A multipurpose advanced material.* Carbohydrate Polymers, 2013. **98**(2): p. 1585-1598.
12. Maria, L., et al., *Preparation and Antibacterial Activity of Silver Nanoparticles Impregnated in Bacterial Cellulose.* Polimeros-ciencia E Tecnologia - POLIMEROS, 2010. **20**.
13. Ul-Islam, M., T. Khan, and J.K. Park, *Water holding and release properties of bacterial cellulose obtained by in situ and ex situ modification.* Carbohydrate Polymers, 2012. **88**(2): p. 596-603.
14. Sintharm, P., et al., *Bacterial cellulose reinforced with skim/fresh natural rubber latex for improved mechanical, chemical and dielectric properties.* Cellulose, 2022. **29**(3): p. 1739-1758.
15. Taokaew, S., M. Phisalaphong, and B.-m. Zhang Newby, *Bacterial Cellulose: Biosyntheses, Modifications, and Applications*. 2016. p. 255-283.
16. Phomrak, S., et al., *Natural Rubber Latex Foam Reinforced with Micro- and Nanofibrillated Cellulose via Dunlop Method.* Polymers, 2020. **12**(9): p. 1959.
17. Bruna, T., et al., *Silver Nanoparticles and Their Antibacterial Applications.* Int J Mol Sci, 2021. **22**(13).

18. Jeevanandam, J., et al., *Synthesis approach-dependent antiviral properties of silver nanoparticles and nanocomposites.* Journal of Nanostructure in Chemistry, 2022. **12**(5): p. 809-831.
19. Yang, G., et al., *Hydrothermal synthesis of bacterial cellulose/AgNPs composite: A "green" route for antibacterial application.* Carbohydrate Polymers, 2012. **87**(4): p. 2482-2487.
20. Hestrin, S. and M. Schramm, *Synthesis of cellulose by Acetobacter xylinum. II. Preparation of freeze-dried cells capable of polymerizing glucose to cellulose.* The Biochemical journal, 1954. **58**(2): p. 345-352.
21. Islam, M.U., et al., *Strategies for cost-effective and enhanced production of bacterial cellulose.* Int J Biol Macromol, 2017. **102**: p. 1166-1173.
22. Kirdponpattara, S., et al., *Structural modification and characterization of bacterial cellulose–alginate composite scaffolds for tissue engineering.* Carbohydrate Polymers, 2015. **132**: p. 146-155.
23. Ross, P., R. Mayer, and M. Benziman, *Cellulose Biosynthesis and Function in Bacteria.* Microbiological reviews, 1991. **55**: p. 35-58.
24. Zhang, H., et al., *Review of Electrically Conductive Composites and Films Containing Cellulosic Fibers or Nanocellulose.* Bioresources, 2019. **14**.
25. Dahman, Y., *Nanostructured Biomaterials and Biocomposites from Bacterial Cellulose Nanofibers.* Journal of nanoscience and nanotechnology, 2009. **9**: p. 5105-22.
26. Cannon, R.E. and S.M. Anderson, *Biogenesis of bacterial cellulose.* Crit Rev Microbiol, 1991. **17**(6): p. 435-47.
27. Gupta, M., *Polymer composite*. 2007: New Age International.
28. Lee, K.-Y., et al., *On the use of nanocellulose as reinforcement in polymer matrix composites.* Composites Science and Technology, 2014. **105**.
29. Feng, Y., et al., *A mechanically strong, flexible and conductive film based on bacterial cellulose/graphene nanocomposite.* Carbohydrate Polymers, 2012. **87**: p. 644–649.
30. Courchene, C., G. Peter, and J.D. Litvay, *Cellulose Microfibril Angle as a Determinant of Paper Strength and Hygroexpansivity in Pinus Taeda L.* Wood and Fiber Science, 2006. **38**: p. 112-120.
31. Li, T., et al., *Developing fibrillated cellulose as a sustainable technological material.* Nature, 2021. **590**(7844): p. 47-56.
32. Lahiri, D., et al., *Bacterial Cellulose: Production, Characterization, and Application as Antimicrobial Agent.* Int J Mol Sci, 2021. **22**(23).
33. Islam, M.U., et al., *Strategies for cost-effective and enhanced production of bacterial cellulose.* International Journal of Biological Macromolecules, 2017. **102**: p. 1166-1173.
34. Watanabe, K., et al., *Acetobacter xylinum mutant with high cellulose productivity and an ordered structure.* Bioscience, biotechnology, and biochemistry, 1998. **62**(7): p. 1290-1292.
35. Keshk, S. and K. Sameshima, *The utilization of sugar cane molasses with/without the presence of lignosulfonate for the production of bacterial cellulose.* Appl Microbiol Biotechnol, 2006. **72**(2): p. 291-6.
36. Hong, F. and K. Qiu, *An alternative carbon source from konjac powder for enhancing production of bacterial cellulose in static cultures by a model strain*

Acetobacter aceti subsp. xylinus ATCC 23770. Carbohydrate Polymers, 2008. **72**(3): p. 545-549.
37. Huang, C., et al., *Using wastewater after lipid fermentation as substrate for bacterial cellulose production by Gluconacetobacter xylinus.* Carbohydrate Polymers, 2016. **136**: p. 198-202.
38. Bielecki, S., et al., *Biopolymers Online*. 2005, Wiley-VCH Verlag GmbH & Co. KGaA Weinheim, Germany:.
39. Stumpf, T.R., et al., *In situ and ex situ modifications of bacterial cellulose for applications in tissue engineering.* Materials Science and Engineering: C, 2018. **82**: p. 372-383.
40. Yan, Z., et al., *Biosynthesis of bacterial cellulose/multi-walled carbon nanotubes in agitated culture.* Carbohydrate Polymers, 2008. **74**(3): p. 659-665.
41. Yoon, S.H., et al., *Electrically Conductive Bacterial Cellulose by Incorporation of Carbon Nanotubes.* Biomacromolecules, 2006. **7**(4): p. 1280-1284.
42. Zhang, X.F., et al., *Silver Nanoparticles: Synthesis, Characterization, Properties, Applications, and Therapeutic Approaches.* Int J Mol Sci, 2016. **17**(9).
43. Zenaida Guerra, Q., et al., *Application of Silver Nanoparticles for Water Treatment*, in *Silver Nanoparticles*, M. Khan, Editor. 2018, IntechOpen: Rijeka. p. Ch. 5.
44. Beck, F., M. Loessl, and A.J. Baeumner, *Signaling strategies of silver nanoparticles in optical and electrochemical biosensors: considering their potential for the point-of-care.* Microchimica Acta, 2023. **190**(3): p. 91.
45. Hussein, H.A. and M.A. Abdullah, *Novel drug delivery systems based on silver nanoparticles, hyaluronic acid, lipid nanoparticles and liposomes for cancer treatment.* Applied Nanoscience, 2022. **12**(11): p. 3071-3096.
46. Iravani, S., et al., *Synthesis of silver nanoparticles: chemical, physical and biological methods.* Res Pharm Sci, 2014. **9**(6): p. 385-406.
47. Demchenko, V., et al., *Effect of the type of reducing agents of silver ions in interpolyelectrolyte-metal complexes on the structure, morphology and properties of silver-containing nanocomposites.* Scientific Reports, 2020. **10**(1): p. 7126.
48. Pal, S., et al., *Silver-Functionalized Bacterial Cellulose as Antibacterial Membrane for Wound-Healing Applications.* ACS Omega, 2017. **2**(7): p. 3632-3639.
49. Mutiara, T., et al., *Facile route of synthesis of silver nanoparticles templated bacterial cellulose, characterization, and its antibacterial application.* Green Processing and Synthesis, 2022. **11**(1): p. 361-372.
50. Salama, A., et al., *Cellulose-Silver Composites Materials: Preparation and Applications.* Biomolecules, 2021. **11**(11).
51. *Creation of composites of bacterial cellulose and silver nanoparticles: evaluation of antimicrobial activity and cytotoxicity.* International Journal of Nanotechnology, 2019. **16**(6-10): p. 408-420.
52. Yang, G., et al., *Preparation and characterization of BC/PAM-AgNPs nanocomposites for antibacterial applications.* Carbohydrate Polymers, 2015. **115**: p. 636–642.
53. Seesuriyachan, P., et al. *Exopolysaccharide production by Lactobacillus*

confusus TISTR 1498 using coconut water as an alternative carbon source: the effect of peptone, yeast extract and beef extract. 2011.
54. Yang, Y., et al., *Nanoporous cellulose membrane doped with silver for continuous catalytic decolorization of organic dyes.* Cellulose, 2018. **25**(4): p. 2547-2558.
55. Escárcega-González, C.E., et al., *Bacterial Exopolysaccharides as Reducing and/or Stabilizing Agents during Synthesis of Metal Nanoparticles with Biomedical Applications.* International Journal of Polymer Science, 2018. **2018**: p. 7045852.
56. Lei, J., A. McClelland, and T.H. Zeng. *Synthesis of Silver Nanoparticles by Vitamin C for Public Health Applications*. in *2022 IEEE 22nd International Conference on Nanotechnology (NANO)*. 2022.
57. Han, Y., et al., *Reductant-Free Synthesis of Silver Nanoparticles-Doped Cellulose Microgels for Catalyzing and Product Separation.* ACS Sustainable Chemistry & Engineering, 2016. **4**(12): p. 6322-6331.
58. Kulikouskaya, V., et al., *Chitosan-capped silver nanoparticles: A comprehensive study of polymer molecular weight effect on the reaction kinetic, physicochemical properties, and synergetic antibacterial potential.* SPE Polymers, 2022. **3**(2): p. 77-90.
59. Kingkaew, J., et al., *Effect of molecular weight of chitosan on antimicrobial properties and tissue compatibility of chitosan-impregnated bacterial cellulose films.* Biotechnology and Bioprocess Engineering, 2014. **19**(3): p. 534-544.
60. Kim, J., et al., *Preparation and characterization of a Bacterial cellulose/Chitosan composite for potential biomedical application.* Journal of Polymer Research, 2011. **18**(4): p. 739-744.
61. Menichetti, A., et al., *Effect of Size, Shape and Surface Functionalization on the Antibacterial Activity of Silver Nanoparticles.* Journal of Functional Biomaterials, 2023. **14**(5): p. 244.
62. Lee, K.-S. and M.A. El-Sayed, *Gold and Silver Nanoparticles in Sensing and Imaging: Sensitivity of Plasmon Response to Size, Shape, and Metal Composition.* The Journal of Physical Chemistry B, 2006. **110**(39): p. 19220-19225.
63. Bolla, P.A., et al., *Synthesis and Catalytic Application of Silver Nanoparticles Supported on Lactobacillus kefiri S-Layer Proteins.* Nanomaterials (Basel), 2020. **10**(11).
64. Zhu, C., et al., *Kombucha-synthesized bacterial cellulose: preparation, characterization, and biocompatibility evaluation.* J Biomed Mater Res A, 2014. **102**(5): p. 1548-57.
65. Jyoti, K., M. Baunthiyal, and A. Singh, *Characterization of silver nanoparticles synthesized using Urtica dioica Linn. leaves and their synergistic effects with antibiotics.* Journal of Radiation Research and Applied Sciences, 2016. **9**(3): p. 217-227.
66. Cui, Q., et al., *Selective oxidation of bacterial cellulose by NO2–HNO3.* RSC Advances, 2014. **4**(4): p. 1630-1639.
67. Mugesh, S., T. Kumar, and M. Murugan, *An unprecedented bacterial cellulosic material for defluoridation of water.* RSC Advances, 2016. **6**.
68. Song, S., et al., *Antibacterial polyvinyl alcohol/bacterial cellulose/nano-silver*

hydrogels that effectively promote wound healing. Materials Science and Engineering: C, 2021. **126**: p. 112171.
69. Sarkar, D., et al., *Three Dimensional Ag2O/TiO2 Type-II (p–n) Nanoheterojunctions for Superior Photocatalytic Activity.* ACS Applied Materials & Interfaces, 2013. **5**(2): p. 331-337.
70. Supanakorn, G., S. Taokaew, and M. Phisalaphong, *Multifunctional Cellulosic Natural Rubber and Silver Nanoparticle Films with Superior Chemical Resistance and Antibacterial Properties.* Nanomaterials (Basel), 2023. **13**(3).
71. Cai, Z. and J. Kim, *Bacterial cellulose/poly(ethylene glycol) composite: characterization and first evaluation of biocompatibility.* Cellulose, 2010. **17**(1): p. 83-91.
72. Gleadall, A., *9 - Mechanical properties of biodegradable polymers for medical applications*, in *Modelling Degradation of Bioresorbable Polymeric Medical Devices*, J. Pan, Editor. 2015, Woodhead Publishing. p. 163-199.
73. Teixeira, S., et al., *Biosynthesis and Functionalization of Bacterial Cellulose Membranes with Cerium Nitrate and Silver Nanoparticles.* Materials Research, 2019. **22**.
74. Mohammadkazemi, F., M. Azin, and A. Ashori, *Production of bacterial cellulose using different carbon sources and culture media.* Carbohydrate Polymers, 2015. **117**: p. 518-523.
75. de Araújo Júnior, A.M., et al., *Regenerated cellulose scaffolds: Preparation, characterization and toxicological evaluation.* Carbohydrate Polymers, 2016. **136**: p. 892-898.
76. Diab, M.A., A.Z. El-Sonbati, and D.M.D. Bader, *Thermal stability and degradation of chitosan modified by benzophenone.* Spectrochimica Acta Part A: Molecular and Biomolecular Spectroscopy, 2011. **79**(5): p. 1057-1062.
77. Watanabe, K., et al., *Structural Features and Properties of Bacterial Cellulose Produced in Agitated Culture.* Cellulose, 1998. **5**(3): p. 187-200.
78. Gelin, K., et al., *Characterization of water in bacterial cellulose using dielectric spectroscopy and electron microscopy.* Polymer, 2007. **48**(26): p. 7623-7631.
79. Zawadzka, K., et al., *Surface area or diameter - Which factor really determines the antibacterial activity of silver nanoparticles grown on TiO2 coatings?* New J. Chem., 2014. **38**.
80. Wu, J., et al., *In situ synthesis of silver-nanoparticles/bacterial cellulose composites for slow-released antimicrobial wound dressing.* Carbohydr Polym, 2014. **102**: p. 762-71.
81. Yin, I.X., et al., *The Antibacterial Mechanism of Silver Nanoparticles and Its Application in Dentistry.* Int J Nanomedicine, 2020. **15**: p. 2555-2562.
82. Khorrami, S., et al., *Selective cytotoxicity of green synthesized silver nanoparticles against the MCF-7 tumor cell line and their enhanced antioxidant and antimicrobial properties.* Int J Nanomedicine, 2018. **13**: p. 8013-8024.
83. Kingkaew, J., et al., *Biocompatibility and Growth of Human Keratinocytes and Fibroblasts on Biosynthesized Cellulose–Chitosan Film.* Journal of Biomaterials Science, Polymer Edition, 2010. **21**(8-9): p. 1009-1021.

VITA

NAME	Ratchanon Jenkhongkarn
DATE OF BIRTH	11 April 1998
PLACE OF BIRTH	Thailand
INSTITUTIONS ATTENDED	CHULALONGKORN UNIVERSITY Bachelor of Engineering in Chemical Engineering
HOME ADDRESS	99/472 หมู่ 4 หมู่บ้าน สีวลี-สุวรรณภูมิ ซอย 3/6 ถนน กิ่งแก้ว-บางพลี (99/472 Sivalee Suwannabhumi Village, Kingkaew-Bangplee Rd.)
PUBLICATION	Jenkhongkarn, R.; Phisalaphong, M. Effect of Reduction Methods on the Properties of Composite Films of Bacterial Cellulose-Silver Nanoparticles. Polymers 2023, 15, 2996. https://doi.org/10.3390/polym15142996